NON-INTRUSIVE MEASUREMENT OF TEMPERATURE DISTRIBUTION IN THE ENGINE CYLINDER AND ITS EFFECT ON KNOCKING PHENOMENA

エンジン筒内温度分布の非接触計測と
ノッキング現象に与える影響

SEPTEMBER, 2015

NUR SAIFULLAH BIN KAMARRUDIN

A Thesis for the Degree of Ph.D in Engineering

NON-INTRUSIVE MEASUREMENT OF TEMPERATURE DISTRIBUTION IN THE ENGINE CYLINDER AND ITS EFFECT ON KNOCKING PHENOMENA

エンジン筒内温度分布の非接触計測と ノッキング現象に与える影響

September, 2015

Graduate School of Engineering

Gifu University, Japan

Nur Saifullah bin Kamarrudin

NON-INTRUSIVE MEASUREMENT OF TEMPERATURE DISTRIBUTION IN THE ENGINE CYLINDER AND ITS EFFECT ON KNOCKING PHENOMENA

by

NUR SAIFULLAH BIN KAMARRUDIN

A thesis submitted in partial

fulfillment of the requirements for the degree of

Doctor of Philosophy

Supervised by

Professor Shuhei Takahashi

Graduate School of Engineering

(Doctor Course)

GIFU UNIVERSITY

JAPAN

SEPTEMBER, 2015

by

Nur Saifullah bin Kamarrudin

CONTENTS

LIST OF TABLES

LIST OF FIGURES

ACKNOWLEDGMENT

In the name of Allah, the Most Gracious and the Most Merciful

Shukur Alhamdulillah. I praise and thank you to Allah Almighty for making it possible for me to come here at Gifu University, Japan, granting me the prosperity to work on a research field that I've dreamed of. All the hurdles and difficulties during this work were only able to overcome by only from His permission.

Deepest appreciation and gratitude for the help and support are extended to every person who in one way or another have contributed in making this study possible.

First of all, I would like to express my special appreciation and thanks to my advisor, Professor Dr. Shuhei Takahashi. You have been a tremendous mentor for me. I would like to thank you for encouraging my research and for allowing me to grow as a research scientist. Your advices on both research as well as on my social life have been priceless. I am honoured to have such a generous doctoral advisor. I would also like to express my sincerest appreciation to Assoc. Professor Tadayoshi Ihara for his valuable advices and guidance during this research.

A big thank you to my committee members; Professor Dr. Yoshinori Itaya, Professor Dr. Nobusuke Kobayashi & Professor Dr. Masaharu Komiyama for serving as my committee members during hardship. Thank you for letting my defenses to be the most enjoyable moments, and for your brilliant comments and suggestions that helped to improve this thesis.

A special thanks towards my family during this journey for their love and flowing encouragement. Words cannot express how grateful I am to my late father, my mother, my mother-in-law, father-in-law and my relatives for all of the sacrifices that you've made on my behalf. Your prayer for me was what sustained me to this far. I would like express special gratefulness to my beloved wife Mrs. Harziatul Fadzlina Haris who gave up her own dreams only to spent time with me in Japan, and was always supported me through her unconditional love. I would like to extend my special appreciation to my beloved kids, Nur Insyirah Hani and Nur Iman Safiyya for always cheering my life, making me smile, and for understanding during those weekends when I have to spend time on this present work instead of playing with them.

I would also like to thank all of my friends who supported me in this writing, and incented me to strive towards my goal. A big thank you to Mr. Shogo Tanaka, Mr. Yoshiaki Takahashi, Mr. Daichi Funai and Mr. Hiroki Shinotani through the years for not giving up doing experiments together to provide precise data. Thank you to all of my colleagues in Combustion Laboratory (Takahashi Lab) for sharing thoughts and supporting me throughout these years.

Not to forget, I am thankful to Malaysian Government under Ministry of Education Malaysia (previously Ministry of Higher Education Malaysia) and Universiti Malaysia Perlis for providing financial support for this work to succeed.

ABSTRACT

Homogenous charge combustion ignition (HCCI) engine operates by combining idea of mixing fuel and air in homogeneous manner outside combustion chamber like the gasoline engines, and the idea of auto-ignition combustion due to high compression air fuel mixture like in the diesel engines. HCCI engine proposed auto-ignition of leaner equivalence ratio (ER) of air-fuel mixture to achieve higher combustion efficiency, yet at the same time produce lower exhaust gas emission. However, the drawback of any auto-ignition engine is that it is sensitive to knock if the heat release occurs at rapid rate, which usually observe when the engine operates at high load. Knock is a phenomenon that should be avoided in internal combustion engine (ICE). It limits the operation range or engine revolution at high speed of HCCI engine. Even with extensive knowledge gained regarding knock behavior studies in recent year, the origin of knock is still not clear. It is known that the occurrence of knock depends on compression ratio, namely the compression temperature. Here, the compression temperature is referred to the mean temperature of gas mixture across combustion chamber. However, knocking repeatability was not guaranteed, especially at critical condition. Recent study shows that there was temperature distribution inside cylinder after the compression completed. Therefore, the understanding of temperature distribution instead of mean temperature is then suggested for controlling auto-ignition phase in HCCI engine.

The purposes of this present study are as follows:

1. To develop a 2D gas temperature measurement system inside the engine cylinder during auto-ignition process by applying infrared (IR) emission method. The developed system then will be evaluated in both non-combustion and combustion situation for the accuracy measurement.
2. To measure temperature distribution inside the engine cylinder when fuel concentration gradient (FCG) is applied, and then to clarify the behavior of cool flame and hot flame during auto-ignition process.
3. To discuss the effect of FCG and temperature distribution on reducing the knock intensity.

A rapid compression machine (RCM) has been used in the present study to demonstrate concept of a HCCI engine. N-heptane is used as fuel and compression ratio ranges from 10 to 12. The air-fuel charge is supplied into the combustion chamber located horizontally. The initial pressure and temperature were maintained throughout in this study as 0.101 MPa and 298 K. Compression of the charge completed in approximately 30 ms, which corresponded to engine rotation speed of 1000 rpm. Once compression is completed, the piston is maintained at the top dead center (TDC) position so that chemical kinetic reaction in cylinder occurred in constant volume condition. For temperature measurement with infrared emission method, a small amount of CO_2 (4.0 vol %) as IR emitter medium is doped into the cylinder prior compression. A high-speed IR camera is placed in front of the combustion chamber (the piston located horizontally) so that the measurement area is at the top of the piston crown. Captured radiation from CO_2 is finally converted to the gas temperature. In the present study, gas mixture is introduced inside cylinder in both homogeneous and inhomogeneous manner.

Obtained results in this study can be summarized as follows:

a) In the case of compression in homogeneous manner,

1. The measured temperature of the non-reacting charge with varying experiment parameters (compression ratios and specific heat capacities) agreed with the theoretical estimation. The developed temperature measurement technique could distinguish the temperature difference about 10K. Additionally the characteristic temperature distribution due to the movement of the piston called a roll up vortex was successfully captured. The results showed that the temperature at the roll up vortex region was 10-30K lower than the core temperature.
2. The temporal behavior of the temperature profile of the reacting charge in the cylinder during the ignition delay was successfully captured. Not only the temperature change due to the appearance of cool flame but the gradual temperature increase during the low temperature reaction are captured

quantitatively as two-dimensional information. Such information is useful for interpretation of the auto-ignition phenomena of the compressed charge.

b) For the case of compression in inhomogeneous (fuel concentration gradient applied) manner,

1. Applying an FCG in the cylinder prior to the compression created temperature distribution in the charge after the process. The compressed charge have high temperature at the leaner mixture and low temperature at the richer mixture in the cylinder due to the difference in the ratio of the specific heat capacities in the two regions. The developed temperature measurement technique could capture the temperature profile in the compressed charge.
2. In all conditions of the present study, due to the temperature distribution, the cool flame started from the leaner part and moved to the richer part, since the low temperature oxidation occurred in the stratified charge successively. The pressure rise owing to the low temperature oxidation became gradual owing to the stratified ignition delay.
3. After the stratified ignition of the low temperature oxidation, a relatively large temperature difference existed in the charge, and the high temperature oxidation then started. The starting point of the hot flame depended on the magnitude of $\Delta\emptyset$ of the FCG. When $\Delta\emptyset$ was small, the hot flame moved from the top to the bottom (as did the cool flame). In contrast, when $\Delta\emptyset$ was large, the hot flame moved from the bottom to the top. There is a critical of FCG ($\Delta\emptyset cr$) at which the total ignition delays for each of the local points became close to each other.
4. The stratified occurrence of high temperature oxidation reduced the KI. With increasing $\Delta\emptyset$, KI will first decrease but then increased at $\Delta\emptyset cr$. Further increases in $\Delta\emptyset$ led to further KI decreases. However, excessively large $\Delta\emptyset$ changes caused incomplete combustion, which resulted in diminish maximum pressure.

1. Introduction

1.1 Motivation

The awareness of global warming phenomenon have push many thermal energy related product developers at both R&D and industries level to produce environment friendly products, especially the internal combustion engine (ICE). Pollutants from vehicle engines are one of the main contributors to the global warming phenomenon. Therefore, strict environment regulations are implemented every year, and it had put great pressure on the industries and researchers to develop and apply environment friendly technologies in vehicles.

In a diesel engine, an air-fuel charge is compressed with high compression ratio to achieve in the auto-ignition combustion process, which contributed higher thermal efficiency over a wide load operating range. This burning process in diesel engine occurred in diffusion combustion, where the air-fuel gas undergoes burning process while mixing process still took place. Combustion in diesel engine start at near stoichiometric air-fuel ratio (yield high combustion temperature) and then the combustion spread in

whole cylinder therefore consume air-fuel charge from lean to rich equivalence ratio (ER) region. Therefore, the nitrogen oxides (NOx) that almost formed in high temperature combustion field and in particulate matter (PM) generated in fuel rich field (where the temperature field is low) are difficult to avoid simultaneously. The gasoline engine, on the other hand faced difficulties to operate in high compression ratio due to gasoline sensitivity to knock occurrence. A leaner mixture of the air-fuel mixture in gasoline is also not a great solution for gasoline engine as the fuel have lower volatility thus face misfiring problem.

Recently a new design engine, homogeneous charge compression ignition (HCCI) engine is proposed to overcome low thermal efficiency in gasoline engine and exhaust gas pollutant from NOx or PM from diesel engine. Concept operating mechanism of HCCI is like combination of operating principle of those two engines, where mixture is introduced into cylinder in homogeneous manner (as in gasoline engine or spark ignition (SI) engine), and then combustion is completed by auto-ignition mechanism (high compression combustion same as in diesel engine or compression ignition (CI) engine). From theoretical point of view, high compression combustion with leaner mixture produced lower combustion temperature, therefore avoid the NOx from being produce. Thus, cleaner exhaust gas due to the combustion process takes place in high temperature field. Additionally, HCCI utilize pre-combustion mixing which helps to avoid locally high region, therby drastically reduce PM formation (Singh *et al.* 2009).

The HCCI engine is still under development process, thus several challenges will be highlighted for this type of engine could be brought into mass production. Auto-ignition process, as the main characteristic of combustion phase in this engine, depends on chemical kinetics reaction of gas mixture inside cylinder once it is being compressed under high pressure. Combustion phase in auto-ignition process may exhibit single or two stages heat release depend on hydrocarbon fuel used. In case of heavy hydrocarbons used as fuel, two stage heat release can be monitored from two times pressure increment in pressure profiles history (Minetti *et al.* 1995, Tanaka 2003), which will be shown in later chapter (Refer Figure 3.10). First heat release is significant with low temperature oxidation (LTO) while the second stage heat release associates with thermal combustion (Griffiths *et al.*

2002). A study using primary reference fuel (PRF) shows that there was strong relation between fuels octane number and heat release in LTO phase. Lower octane number (like in diesel) contributed to noticeable LTO and higher octane number (for example, gasoline) released very low LTO (Tanaka 2003). Consequently, two-stage ignition (two-time pressure increment in pressure profile graph, Figure 3.10) in CI engine with diesel fuel obviously able to distinguish compared the one with gasoline. LTO being studied by many researchers as it suggested have strong influence on knock behavior (Tanaka 2003, Yamada *et al.* 2004, Iijima *et al.* 2010) in CI engine. They agreed that further understanding on LTO might provide knowledge regard controlling auto-ignition timing in CI engine. Other parameters that affect combustion phasing are compression ratio, mixture intake temperature, and also mixture homogeneity.

Controlling ignition timing in HCCI engine is not a simple task be solved. (Tanaka 2003) again conducted an experiment using a RCM to investigate effect of fuel structure and additives to ignition delay and also heat release rate. They stated that the equivalence ratio of PRF such as n-heptane (RON 0) and iso-octane (RON 100) affected the burning rate as well as knock intensity. They also observed that ignition delay, however, is the function of n-heptane to oxygen mole ratio.

Another attempt to control ignition timing was conducted by (Liu *et al.* 2011). They investigated effect of applying temperature inhomogeneities into ignition delay and burning rate using a four-stroke engine simulate HCCI combustion. Temperature inhomogeneities were brought forth by creating different temperature between intake temperature and coolant temperature. Results show that in temperature inhomogeneities, the pressure rise, and heat release rate was able to tone down. Also, combination with piston bowl geometry where it was able to create more turbulent, increased the temperature different in cylinder, which results in different auto-ignition delays.

At early stage of study in basic principles of HCCI engine, initial temperature of gas mixture was set prior compression take place. However, little knowledge was gain in measuring development of temperature post compression process. The attempt to measure gas temperature inside engine started decades ago. (Agnew 1961) applied two band infrared radiation method to measure temperature of water vapor as radiation emitter, and

they chose two different bands i.e. 1.89 and 2.55 microns for measurement purpose. Obtained result showed a good agreement with calculation data under several different operating conditions but limited only in the absent of thermal flame. (McComiskey *et al.* 1993) also conducted a similar study with same water vapor used as emission radiator. The study involved capturing images in cylinder. The experiment setup was able to capture image up to 1800 frame/sec. They selected spectral bands of imaging as 2.2-2.5 micron and 4.5-5.5 micron. Effect of strong radiation from CO_2 near 4.5 micron region was also carefully taken into consideration. The study focused on investigating development of temperature during knock occurrence in reciprocating engine. In the study, they found that no bizarre of local temperature increment in cylinder happened right before knock. However during the knock occurrence, temperature at origin of knock suddenly exhibit large radiation and lasted longer than normal combustion.

In this laboratory experiment simulating HCCI engine, homogenous air-fuel mixture with known equivalence ratio being carefully prepared before auto-ignition compression was conducted. With this homogeneous air-fuel mixture, many experiments were conducted to monitor the effect of various fuel properties to combustion behavior such as ignition delay, heat release rate and knock intensity in HCCI engine. However in practical continuous running HCCI engine, it was almost impossible to have a complete homogeneous gas mixture at every cycle. Research conducted in one single shot compression like in RCM showed that there was aerodynamic effect existed even in simplest geometric features inside cylinder after compression completed (Mittal and Sung 2006). Roll up vortex phenomenon, which was one of aerodynamic effect, clearly showed that inhomogeneous gas mixture developed after the compression complete. Therefore, in order to have a better understanding of HCCI engine, it also necessary to consider the effect of inhomogeneous equivalence ratio in auto-ignition combustion after the behavior of auto-ignition combustion phase in homogeneous manner is established.

Effect of stratified mixture (inhomogeneous) and turbulence in HCCI engine to the ignition delay and emission was studied and it proved that stratified mixture and turbulence can be utilized for controlling auto-ignition timing and combustion process. Previous study in our lab also proved that applying inhomogeneous in cylinder was able

to lower the knock intensity without sacrificing maximum pressure (Xiaojian *et al.* 2006, Ihara *et al.* 2007). (Thirouard *et al.* 2005) conducted an experiment to optically monitor effect of applying inhomogeneous mixture. An optical access was placed on top of engine to monitor ignition of flame front. Inhomogeneous mixture was then produced by using multiple direct injections. From the study, it can be concluded that thermal flame tend to ignite at location where equivalence ratio was at rich region.

Based on all explanation above, it is believed that the first stage heat release during LTO process contributed in controlling time of auto-ignition. Modifying inhomogeneous mixture is able to extend load operation limit of HCCI engine. Inhomogeneous gas mixture will affect a non-uniformity temperature after compression complete. However, there is still not clear how inhomogeneous mixture contribute to this improvement. Optical temperature measurement tool is proposed to monitor the distribution of temperature inside cylinder. The relation of temperature growth inside cylinder to the LTO and thermal heat also being observed. Several attempts at measuring gas temperature inside cylinder by experimental and numerical methods were conducted to achieve better understanding of combustion process (Yao *et al.* 2009).

Recent developments in optical apparatus allow the possibility to capture precise temperature. Therefore a high-speed infrared (HSIR) camera is suggested to monitor optically combustion phase in cylinder. Challenges in measuring temperature in cylinder are highlighted in latter chapter. The study was undertaken to measure temperature distribution in cylinder starting from compression complete at top dead center (TDC), during development of low temperature oxidation (LTO) until the appearance of thermal flame. Comparison between measured temperatures compressed in homogeneous manner with theoretical calculation was conducted earlier for determining accuracy of the experiment setup. Once the developed measurement became reliable, temperature measurement of inhomogeneous stratified gas mixture was then being proceeded. Temperature growth inside cylinder was closely monitored by HSIR camera, and being synchronized with pressure profiles to explain relation between experimental parameter with temperature distribution growth during auto-ignition combustion phase. Effect of

apply temperature distribution in cylinder to the behavior of knock phenomenon during auto ignition also was tried to be explained in this study.

Finally, a chemical reaction simulation software, CHEMKIN-PRO was used to explain the behavior of LTO and thermal flame in stratified gas mixture CI. A multi zone model reactor was adapted to simulate inhomogeneous mixture in HCCI engine. Simulation condition apply several value of experiment condition such as initial pressure, initial temperature and also compression ratio. Simulation result successfully re-demonstrate behavior of LTO and hot flame that conducted in experiment.

2. Literature review

In this chapter, a literature review is based on present study of the title "Non-intrusive measurement of temperature distribution in the engine cylinder and its effect on knocking phenomena". The literature review was divided into three main sub-chapters i.e.:

1. Intrusive and non-intrusive measurement method.
2. Temperature distribution / fuel concentration gradient (FCG) in internal combustion engine.
3. Effect of temperature distribution and FCG on knock phenomena.

2.1 Review on intrusive and non-intrusive gas temperature measurement method

Knowledge of gas temperature inside internal combustion engine (ICE) is necessary as it is very important especially on the combustion temperature and unburned end gas temperature right before the occurrence of knock. The information is crucial to characterize chemical kinetic process in auto-ignition combustion process. Attempts at

measuring gas temperature in ICE was of interest for many researchers in past few decades. The measurement methods can be divided into two group namely intrusive method and non-intrusive method.

Intrusive method, as it carries with the name was normally involved measurement probe to be direct contact with combustion field, e.g. thermocouple. This method is not preferable due to its effect of combustion field, the probe itself suffer from corrosion if was use for a long period, plus the response is very slow compare with the development of temperature during auto-ignition compression.

Recent development in optical diagnostics allows non-intrusive method to overcome problem stated for intrusive method. The optical diagnostics were not only able to measure combustion temperature with fast response but also measure the flow field and soot particle. For instance, current popular non-intrusive method to measure temperature of combustion are such as laser induced fluorescence (LIF) (Peterson *et al.* 2013), Rayleigh scattering method (Yuen and Gülder 2009), and diode laser absorption method (Mattison *et al.* 2007, Rieker *et al.* 2007). However, these methods require at least two optical windows at the opposite location to allow laser beam passes through to detector, which caused system setup to be complicated as well as high cost of using a laser system. Moreover, these method are still difficult to be applied on high-pressure environment like a combustion chamber of RCM due to the nature of their relatively weak signal. (Hamamoto *et al.* 1994) applied optical interference technique to measure temperature history of unburned end gas during under knock operating condition. They first conducted an experiment in a constant volume combustion chamber for validation purpose. Later, they proceed to next experiment in an engine. Measurement temperature history showed good result with calculated adiabatic temperature. Another non-intrusive measurement method is an infrared method using absorption/radiation medium such as H_2O or CO_2. This method is suitable for internal combustion engine (Moroto *et al.* 1999).

2.1.1 Non-intrusive method: Determination of temperature by infrared radiation

Measurement temperature in high temperature field is essential to seek better understanding of combustion reaction process. It is, therefore able to improve combustion efficiency as well as fuel performance. From the point of radiative transport, infrared radiation constitutes a major part of flame radiation while ultraviolet rays and visible light contribute in a very small part. Amongst spectrographic method, infrared radiation technique is one of the promising method. These three assumptions could establish measuring infrared technique;

a. Radiating gasses in thermal equilibrium.
b. Kirchoff's law is valid for the radiating gasses.
c. There is comparison continuum from a black body emitter or other known standard emitter.

Radiation intensity from a black body is continuous and has a specific spectrum depends on the temperature of the body. In the case of a particular gas, the radiation intensity, however, is banded over a certain wavelength. Strong non-luminous radiation principally exhibits from hydrocarbon fuel combustion burning with air. This principle idea is illustrated in Figure 2.1.

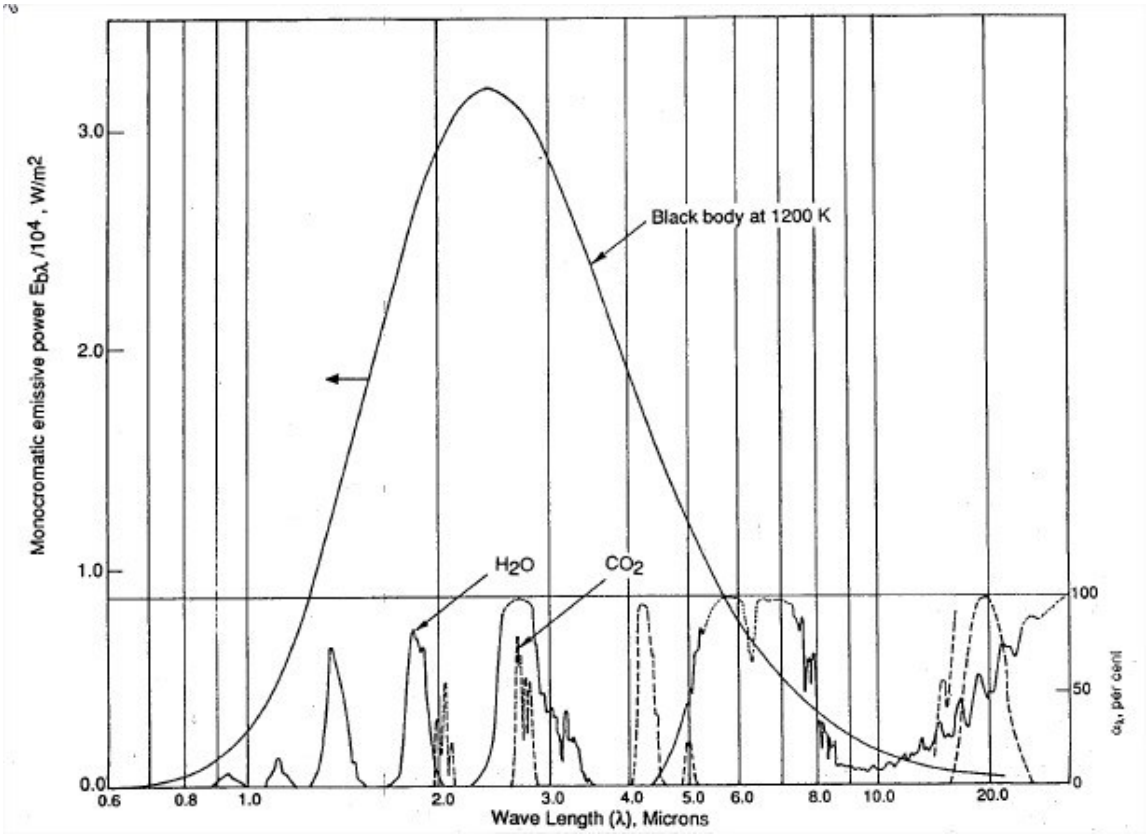

Figure 2.1 Distribution of radiative heat flux for a blackbody source and emission bands for CO_2 and H_2O (Blunsdon *et al.* 1993)**.**

Several attempts at measuring gas temperature from infrared radiation were carried as early in 1950's. (Silverman 1949) applied infrared absorption method to measure flame temperature with three different flames. In his work, he measured temperature based radiation from CO_2 in the 4.2 μm wavelength region. He concluded that the measured temperature were lower compared with the calculated theory due to self-absorption phenomena. However, this result was expected because measuring temperatures at higher frequency weight more on the cooler portion in the flame.

Basic concept of measurement temperature by infrared radiation relies on the fact that, the radiation intensity from any object varies with temperature. (Agnew *et al.* 1955) applied IR emission temperature measurement method in flat burner and try to adopt it in engine. They measured emission release from H_20 and CO_2 species as emitter with several wavelength regions for comparison purposes. (Agnew 1961) again applied the

measurement concept to a reciprocating engine and proposed two-wavelength measurement methods, which required measurement of different known wavelength at one time. Theoretically, the requirement of information on absolute emissivity at particular wavelength was not necessary if the ratio of intensities in the two different wavelengths were known. In this study, they utilized water vapor as a radiating emitter with two different bands, i.e. 1.89 and 2.55 μm.

Another similar experiment was conducted by (McComiskey *et al.* 1993). An experiment was carried out to investigate more on flame propagations. They capture radiation from water vapor with dual band wavelength chose in between 2.2-2.5 and 4.5-5.5 μm. They also conducted experiment in knock condition and their findings based on obtained IR images regarding knock in engine were as follows.

a. Combustion product in the end gas volume upon knock showed no extraordinary behavior like higher temperature compared with no knocking condition.
b. Once knock occurred in engine, emitted radiation will last longer.
c. Combustion product from end gas did not develop higher temperature than other region.

(Jir-Ming and Jun-Hsien 1996) conducted an experiment on measuring open flame temperature with infrared radiation technique. Experiment was done with both premixed and diffusion flame. In this study, they also focused on measured radiation from CO_2 and selected single band i.e. near 4.3μm wavelength region. Measured data with IR technique were compared with two types of thermocouple (S and B type) data for verification. They concluded that the provided data showed a good agreement. The deviation data between IR and thermocouple was below 6% in average error.

Another attempt at measuring temperature based on single wavelength of IR radiation was conducted by (Zhao *et al.* 1991). Measurement target, however, was a solid body which was cylinder head. Even in single wavelength IR radiation absorption method, as long as the calibration method being conducted in proper way, the comparison of

measured temperature between infrared camera and thermocouple showed a good agreement.

2.2 Temperature distribution and fuel concentration gradient in cylinder

As introduced in the previous chapter, a homogeneous mixture of fuel-air is desired for HCCI engine at early stage. In laboratory experiment that use one shot compression system such as shock tube and RCM, one is able to ensure that gas mixture being introduced with homogeneous condition. However, it is almost impossible for a continuous operating reciprocating engine to have a complete homogeneous mixture once it is introduced into combustion chamber. It is due to the effect of aerodynamics inside cylinder during compression, geometry of cylinder itself, and the presence of residual gas from the previous cycle.

Investigation on effect of aerodynamics inside cylinder was conducted by (Mittal and Sung 2006). The experiment was conducted in a rapid compression machine (RCM) and the aerodynamics affect after compression was measured with a planar laser induced fluorescence (PLIF) of acetone. Comparison of the flow inside combustion was done between a flat head piston and a crevice piston. The experiment result showed the compression with flat head piston resulted in significant mixing between of the cold vortex region with hot core region in the middle of cylinder, and it also penetrate roll-up vortex phenomena. Meanwhile, for the creviced piston, gas velocity after the compression was quite lower and hot core region remained unaffected and lasted longer i.e. up to 100 ms after compression.

The presence of the aerodynamics affect and even worse, the appearance of roll up vortex contribute to temperature difference inside cylinder. Comparison between temperature of roll up vortex to the surrounding was investigated by (Clarkson *et al.* 2001) and they found the temperature difference could be up to 50 K. Recently we also (Saifullah *et al.* 2015) found the same phenomena and temperature results was up to 40 K.

Another effort on measuring temperature field in cylinder can be found on (Desgroux *et al.* 1995, 1996).

2.3 Effect of temperature distribution and FCG on combustion and knocking phenomena

Effect of temperature and fuel concentration distribution inside cylinder to combustion phenomena was investigated. (Griffiths et al. 2002) conducted experiments in a RCM to investigate origins of knock in controlled auto-ignition (CAI) or HCCI by using n-pentane as fuel. They found that the origin of knock had a relation with spatially non-uniform development of spontaneous ignition from localized development of kinetic inhomogeneities.

In our previous lab, a study on the effect of fuel concentration gradient (FCG) conducted by (Ihara *et al.* 2007) which applied n-heptane as fuel, and mean equivalence ratio used was ER=0.6, 0.8 and 1.0. The obtained results showed that knock intensity was able to be lower if the gradient applied was larger. Ignition delays of FCG mixtures, however, did not depend on the magnitude of FCG but the mean equivalence ratio applied in cylinder.

Recent study conducted by (Mansfield *et al.* 2015) was to investigate low-temperature ignition of using iso-octane as fuel. The study was carried by both experimental and simulation to predict autoignition behavior as well as ignition delay. The result showed that for lower equivalence ratio i.e. ER=0.25, effect of inhomogeneous was not significant. Richer equivalence ratio (ER=1.0) on the other hand affected the accuracy for prediction of ignition delay become poor for the case of ignition delay longer than 1 ms.

3. Experiment Methodology

In this chapter, explanation regarding experimental apparatus used in this study and measurement of fuel concentration gradient (FCG) will be discussed. This chapter involves assessment of experiment setup therefore preparation of air-fuel mixture in homogeneous manner also will be highlighted.

3.1 Rapid Compression Machine

In this study, a rapid compression machine (RCM) was used to simulate auto-ignition combustion. The cylinder head of RCM modified to allow optical access for measure temperature distribution in the cylinder. RCM have a long history of studying auto-ignition behavior. Even there are another option of experiment method such as motored engine, shock tubes, combustion bomb and flow reactor, RCM has advantages such achievable of high pressure after compression complete, and absent of residual gas.

Although the behavior of the gas motion and the composition of the charge in RCM are different from those in the practical reciprocating engine, RCM can simulate a single compression process and maintain constant volume after compression. Another advantages in RCM that it also allow easy measurements of ignition delay and emission intensity through the optical window. Furthermore, the absence of intake and exhaust valves avoid the complicated gas motions such as swirl or tumble that exist in a practical engine.

Detail explanation and operation on RCM used in this study can be found in (Qin 2007). However, detail cross sectional of cylinder head of RCM are shown in Figure 3.1. The geometry of RCM used here has 65 mm bore and 142 mm stroke. Flathead aluminum piston without crevice at side surface used in this study. Non reflective black color with heat resistant was painted at piston crown so that unnecessary emission reflection could be forefend. Compression ratio (CR) was changeable, mainly set to be 10.0 – 12.0 by replacing with different thickness of a spacer that insert in between sapphire glass and cylinder wall. A sapphire glass was used as an optical window as it able to transmit both visible and infrared emission. Additionally, sapphire glass also has high material strength and able to stand thermal shock resistance therefore it suits the needs in knocking produced experiment in this study. Fuel and CO_2 gas as infrared medium (which will be explained later) was injected through an inlet port located below of cylinder. Air and other diluent gas can be supplied through air/gas mixture inlet port located at above of cylinder.

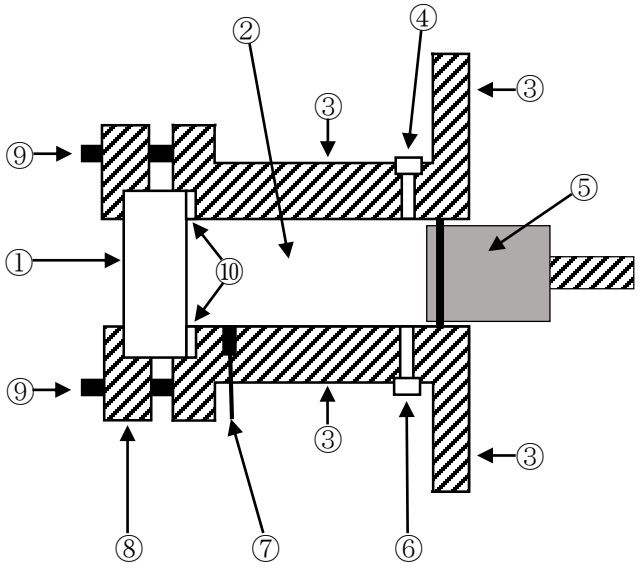

Figure 3.1 Detail parts of cylinder head in Rapid Compression Machine (RCM)

① Sapphire glass

② Combustion chamber

③ Cylinder wall/body

④ Air / diluent gas inlet

⑤ Aluminum piston (with piston ring)

⑥ Fuel / CO_2 injection port

⑦ Pressure probe

⑧ Window glass holder

⑨ Nut & bolts

⑩ Seal & spacer

The arrangement of experimental apparatus was illustrated in Figure 3.2 so that experiment with homogeneous and inhomogeneous condition able to be conducted and optically monitored by both high speed visible light and high speed infrared camera. Charge mixture introduced into combustion chamber and then compressed in adiabatically manner with an aluminum piston driven by high pressure air. The compression time was approximately 30 ms, which correspond to the rotation speed of 1000 rpm in reciprocating engine. A pressure transducer (KISTLER 6052C) was used to monitor the pressure history in the cylinder from the beginning of compression until 30ms after TDC. For temperature measurement, small amount of CO_2 (4.0v %) as the IR emitter medium gas was doped earlier in the cylinder from the inlet port by a micro-syringe. As temperature of gas mixture being developed in cylinder, high speed infrared camera (FLIR SC7000) was used to capture the IR emission released from CO_2 (as an emitter medium) inside combustion chamber, which was finally converted to the temperature. The frame rate of the HSIR camera was 3598 fps. The cell size of the detector was 30μm. The size of measurement area was 85mm x 68mm, which corresponded to 80 x 64 pixels in this thesis. Therefore, the corresponding area for a cell was about 1.1mm square. The radiation from CO_2 was filtered by a narrow band pass filter (center wavelength 4428nm, width ±57nm) located in front of the HSIR. An optical trigger that detects the motion of the piston was used to synchronize the zero-time for both the pressure transducer and the HSIR.

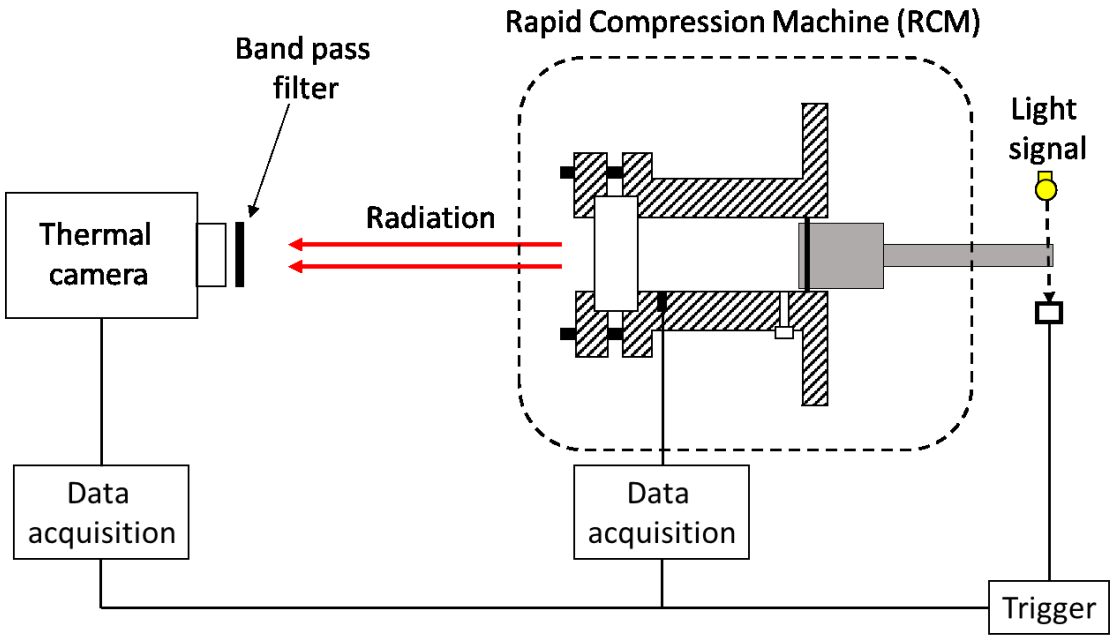

Figure 3.2 Experiment apparatus setup Infrared (IR) emission method

Thermal imaging technique was preferred in this study for local temperature measurement. There are several methods that utilized on infrared radiation as function of temperature changes, which are infrared (IR) absorption method, emission method and absorption-emission method. IR absorption and absorption-emission method require external IR emitter light to provide radiation information, passing through combustion field, therefore, two optical windowing needed in experiment setup. Measuring temperature of solid body is much simpler compared with gas. (Zhao *et al.* 1991) measured cylinder head temperature by transporting emission from below piston crown through one silica window located at side wall of cylinder. (Buono *et al.* 2011) also measure temperature of piston head. Released radiation from a piston was scan with IR photodiode that located inside special spark plug. Unlike with solid body, gas temperature measurement, however, need to set specific known species as it exhibit different pattern of IR radiation. Therefore, earlier solid information on relation of radiation pattern relate with specific species need to be established first. (Agnew *et al.* 1955) applied IR emission temperature measurement method in flat burner and try to adopt in engine. They measured

emission release from H_20 and CO_2 species as emitter with several wavelength region for comparison purpose.

In this study, author chose carbon dioxide (CO_2) as it has strong emission band around 4.3μm and its spectrum profile changes depending on the number density and the temperature. In the emission method, a narrow band pass filter located between camera and RCM (as illustrated in Figure 3.2) to limit range of detected the emitted energy through a narrow band pass filter. The filter is necessary to reduce interfere of other energy at shorter band. Although CO_2 generated in a large portion as hydrocarbon combustion product, target measurement range in this study is between from right after piston reach at top dead center (TDC) until right before appearance of thermal flame. Therefore, compressed mixture undergoing low temperature oxidation (LTO) reaction, does not produce CO_2 in before the thermal flame appears. Thus, CO_2 is a good emitter medium for the temperature measurement. To calculate temperature with the emission method, the database of emitted energy from CO_2 in the relevant ranges of pressure and temperature should be prepared. The radiation spectrum from CO_2 around 4.3μm is due to asymmetric stretching mode of C-O bond.

There have been developed several radiation calculation codes, for example, HITRAN, HITEMP, which are based on line-by-line calculations. The alternative approach is the statistical one, for example, RADCAL (Grosshandler 1993), which uses the narrow band model based on the theory proposed by (MALKMUS 1963). Although line-by-line approach has high resolution, the accuracy at higher temperature (>1000K) is not so good due to the lack of experimental data (Modest 2003). On the other hand, RADCAL is based on the result of combustion experiments and, therefore, its spectrum profile has moderate accuracy even at high temperature (Modest and Bharadwaj 2002). The present emission method depends especially on the shape of the spectrum within the width of the filter but not on the integrated intensity. Hence, RADCAL code is preferable for the present method.

The database used to reconstruct the gas temperature was built by RADCAL, in which the self-absorption by the layers which were located between the detector and the gas under consideration, namely, the effect of the optical thickness was considered properly.

For example, experiment with CR=11, the physical thickness was set to be 14.5 mm, and the optical thickness was calculated by the thickness, pressure and CO_2 concentration. As might expected, the HSIR camera would detect the integral of the intensity along the optical path. Therefore, if the complex distribution exists along the path, it causes reasonable error. In the present study, author assumed that the profile along the path was simple top hat distribution due to the simple geometry of the cylinder.

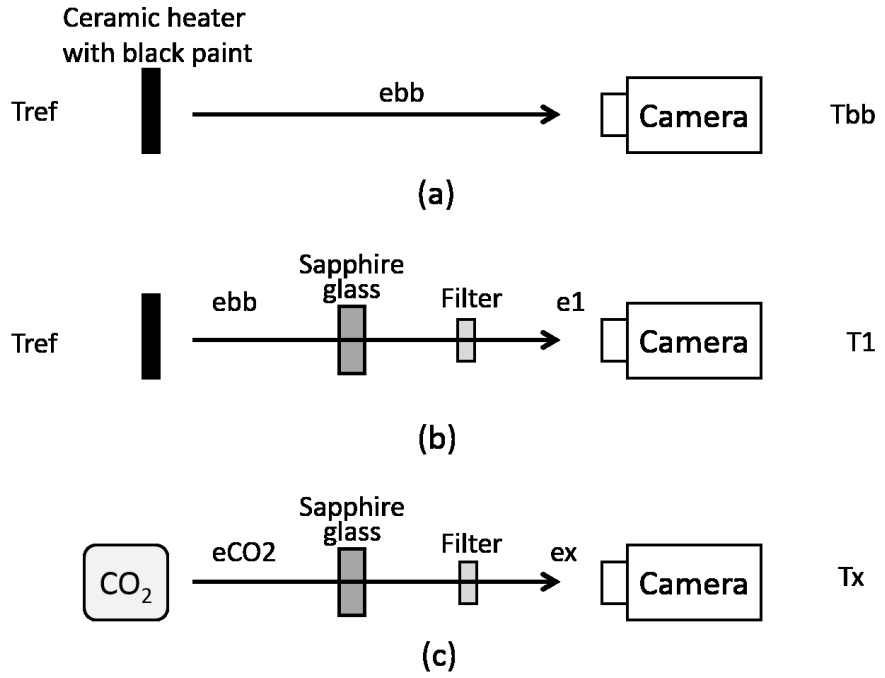

Figure 3.3 Calibration method for measuring emission intensity from CO_2

In order to convert the signal from the IR camera to the gas temperature, the relation between the emission energy and the reported temperature of the HSIR camera used need to be calibrated. Following steps were done to measure HSIR emission and illustrated in Figure 3.3. Direct radiation from simulated black body i.e. a ceramic heater with non-reflective black paint coating was being measured first. A thermocouple was placed behind ceramic heater and connected to the temperature controller in order to keep the heater's temperature steady. The temperatures of the ceramic heater were set to be from

600K – 900K with increasing every 10K. These temperatures labeled as T_{ref}. HSIR then were set to capture the corresponding temperature of the heater, which are labeled as T_{bb}. Emission energy from black body (ceramic heater) at specific temperature can be calculated based on Planck theory, e_{bb}. Since some portion of the emission was absorbed by atmosphere, the reported temperature T_{bb} would result in lower value than T_{ref}. Hence, the relation between actually emitted energy, e_{bb} and the temperature of the heater, T_{ref} will be established first. This above mentioned step is illustrated in Figure 3.3(a).

Next, the same process as mentioned above was repeated, but at this time the sapphire glass and the narrow band pass filter were installed between the light source and HSIR camera as shown in Figure 3.3(b). As expected, recorded temperature in thermal camera is getting much lower as emitted radiation from blackbody was limited by the sapphire glass and the narrow band pass filter. The recorded temperature at from HSIR camera is designated as T_1. The transmittance of the sapphire glass and the narrow band-pass filter were investigated by Fourier transform infrared (FTIR) spectroscopy in advance, therefore the emission energy that reaches the HSIR camera, e_1, could be calculated from e_{bb}. Therefore, new relation between e_1 and T_1 was then obtained, which was be used to estimate the gas temperature.

The process in Figure 3.3(c), shows how the emission energy released from CO_2 gas, e_{CO2} being estimated. Recorded temperature at HSIR camera was named as T_x and the emission captured was noted as e_x. With the relation between e_1 and T_1, emission (e_x) from correspond T_x was able to be calculated. When e_x is known, then e_{CO2} also can be calculated from the transmittances of the glass and the filter. Finally radiation emission of e_{CO2} can be extract from T_x. Once e_{CO2} is known, corresponding temperature of CO_2 can be calculated based on database created from RADCAL code. Therefore, the accuracy of the developed method mainly depended on the model that RADCAL code used, but its validity has confirmed again by (Modest and Bharadwaj 2002).

Previous research done in the same laboratory that conducted by (Nagae *et al.* 2006), they found that when bands located at shorter wave length near 4.2-4.3μm, the absorption of emission energy in the cold boundary layer on the glass became large, which caused considerable error. On the other hand, if the band was set at further wave length, the

intensity at low temperature was so small that cause measurement the temperature profile at low temperature condition could not achieve. Therefore, the band for the measurement should be selected properly according to the temperature and pressure ranges relevant to the measured object. The selected band (center wavelength 4428nm, width ±57nm) is located on the slope where the emission intensity begins to fall off.

Predicted typical spectrum profile of radiation from CO_2 at several given temperatures also effects of doping amount of CO_2 in cylinder (2 vol% and 4 vol%) into the spectral radiance profiles constructed in RADCAL code shows in Figure 3.4 (a) & (b). In the figures also show the transmittance of the band-pass filter used in the experiments. Based on these two figures, 14 experiment parameters (7 different temperature and 2 different concentration of CO_2) were visualized for explanation purpose, however, throughout in this study, about 21,600 constructed data were prepared in advance. All constructed specific spectrum profile then being integrated with transmittance of the band pass filter to predict amount of emission energy collected for each experiment parameters.

HSIR camera captures the emission from the CO_2 that passed through the band-pass filter and the sapphire glass. By integrating the specific spectrum profile at a given temperature with the transmittances of the glass and the band pass filter in Figure 3.4, the amount of emission captured by IR camera, e_x; will be obtained. Figure 3.5 shows an example of the predicted relation between the temperature of CO_2 and the detected infrared intensity for the condition where the initial pressure is 0.101MPa and the CR =10.0. Such curves were calculated from the database with varying the total pressure, CO_2 concentration and the thickness of the clearance volume, which are changed according to the compression ratio and the initial pressure. Based on this information, specific temporal temperature of CO_2 are able to be calculated by inverse calculation based on T_x reported by HSIR camera.

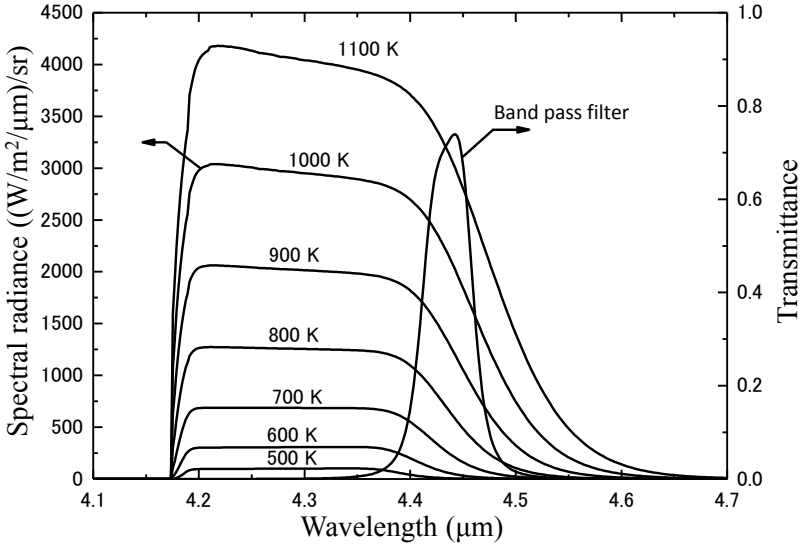

a) 2 vol% of CO_2 doped in cylinder

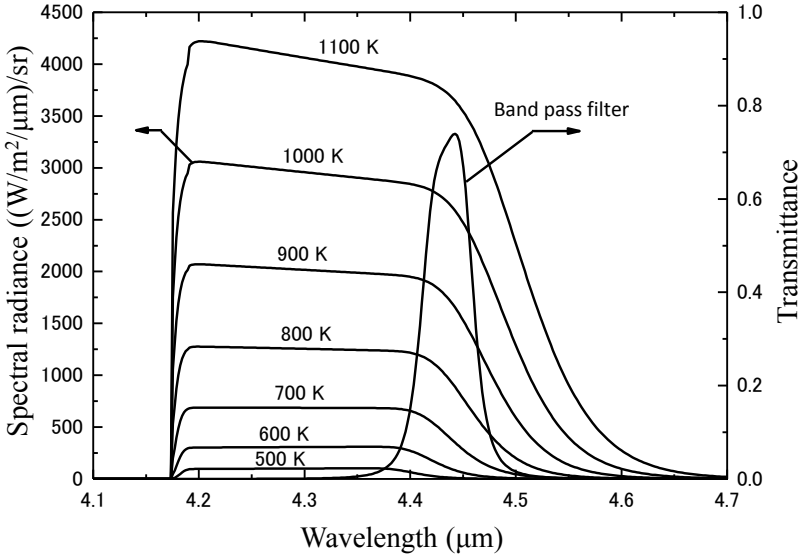

b) 4 vol% of CO_2 doped in cylinder

Figure 3.4 Predicted emission intensity profile from compressed CO_2 at different T. Pi = 0.101 MPa and the CR =10.0

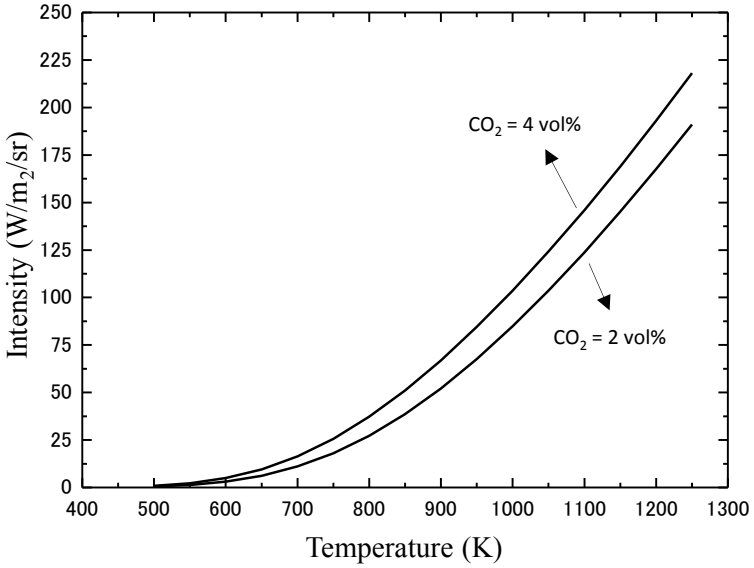

Figure 3.5 Relation between the temperature of CO_2 and the detected infrared intensity though band-pass filter and sapphire window. Pi = 0.101 MPa and the CR =10.0

3.2 Preparation procedure of mixture charge

In this study, author conducted experiments for homogeneous and inhomogeneous condition. Preparation procedure between those two conditions are differs and will be explained here.

3.2.1 Homogeneous Mixture Compression

Arrangement of experiment setup was shown in Figure 3.2. Following steps are the experiment procedure for homogeneous mixture compression:

a. Combustion chamber being put into vacuum condition first. This procedure is important to create basic benchmark condition for measurement purpose and most important is to avoid residual gas if exist.
b. CO_2 gas and fuel (liquid) being insert from bottom of cylinder by a microsyringe. Since inside combustion at the moment is vacuum, once fuel injected it will evaporate in no time, however, care has been taken here so that no fuel was split on piston surface.
c. Air or diluent gas filled in into combustion chamber until desired pressure. A needle valve was used to control volume of air while monitoring pressure inside chamber with a digital manometer. Air will enter in high speed that may cause turbulence inside combustion chamber, which will increase mixing rate of air and fuel. After desired pressure achieved, a valve is closed, and the combustion chamber being leave in this state for 3 minutes. This step is to ensure that flow inside combustion become stable before compression begin.
d. Rapid compression begin and compression complete within approximately 30 ms. Once piston reach foremost (TDC) position, a piston arm locker being set up in position so that it will lock piston from being rebounded back. This step is important to ensure that chemical kinetics reaction in combustion chamber will undergo in equal volume. Here, if the locker arm not able to lock both sides of piston arm, then the experiment will be repeated.

e. Experiment complete. Once all needed data was successfully collected then next experiment preparation will be proceed.

3.2.2 Inhomogeneous (Stratified) Mixture Compression

As mentioned in previous chapter, fuel concentration gradient (FCG) able to lower knock intensity. Therefore, one of main focus of this study is to measure effect of FCG and its effect on temperature distribution growth inside chamber with fuel stratified case. In the experiments, stratified charge was created by injecting the fuel from the bottom part of the cylinder and waiting within controlled time. Experiment preparation steps are similar with mentioned in previous chapter but in different order, i.e. Chapter 3.2.1 (a)→(c)→(b)→(d).

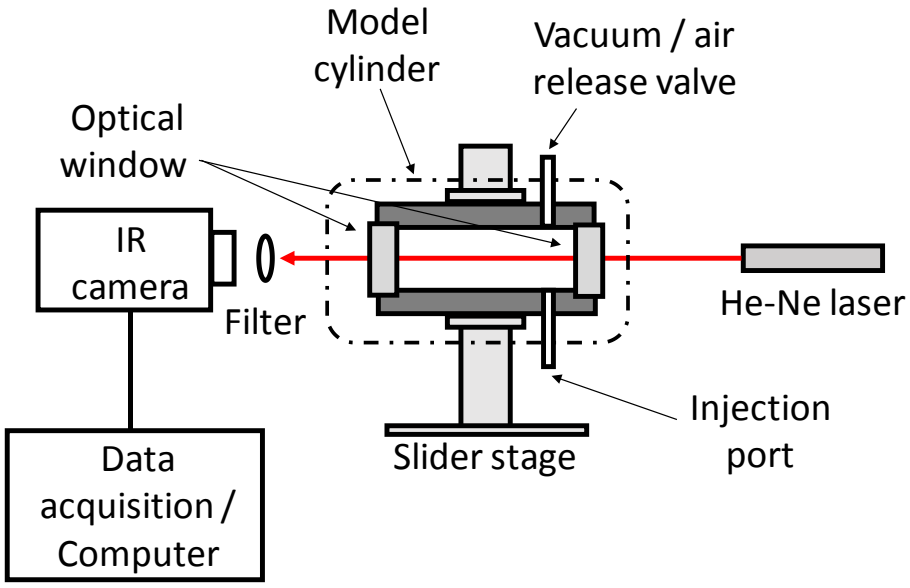

Figure 3.6 Experimental apparatus for measuring growth of fuel concentration gradient.

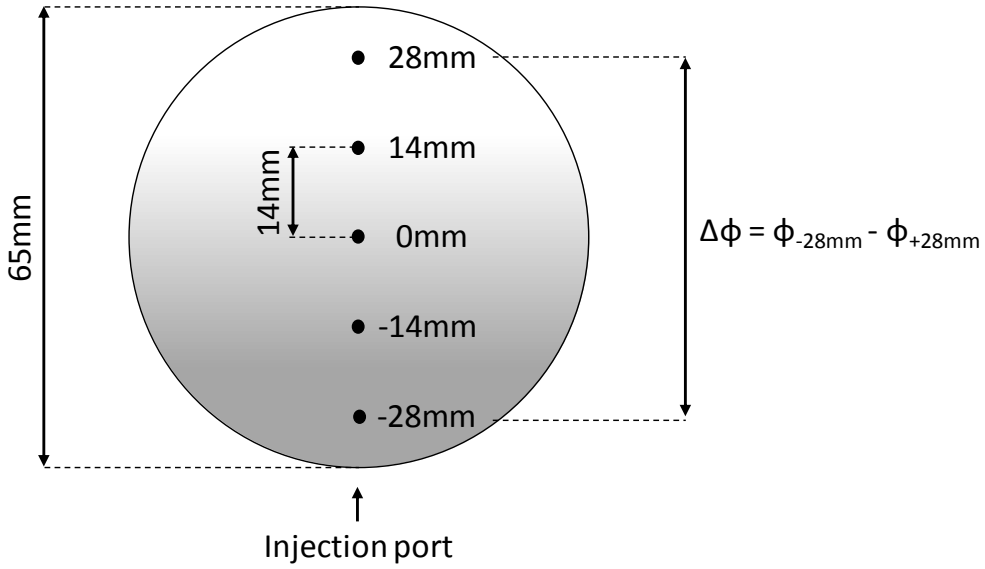

Figure 3.7 Measurement position of local equivalence ratio and definition of fuel concentration gradient.

3.3 Measurement of fuel concentration gradient in combustion cylinder

In creating FCG in the cylinder, it is important to measure and control the local equivalence ratio. Hence, we measured the relationship between the waiting time and the local equivalence ratio profile by infrared laser absorption method in advance. Figure 3.6 shows the experiment apparatus for measurement FCG in the chamber. A model cylinder that had the same dimension of cylinder of RCM was placed on a vertical slider stage. Height of the stage is adjustable to allow model cylinder could be aligned with position of laser as IR light source. The positions of both He-Ne laser (λ=3.39μm) and IR camera were fixed at the same height so that the N/S ratio could be minimized. In order to calculate the local equivalence ratio at a certain elapsed time, Lambert-Beer law was applied to detect the absorption coefficient. The chamber was evaluated by the vacuum pump first, and then the air was introduced at 0.101MPa. After that, the fuel was injected from the injection port at the bottom of cylinder with the syringe pump. A quartz glass was attached to both of end side the model chamber to allow the laser beam access, therefore, absorbed intensity able to be detected by the IR camera. Five different observation locations (±28mm, ±14mm and 0mm from center of cylinder) shown in Figure 3.7 were decided to measure the temporal change of the local equivalence ratio.

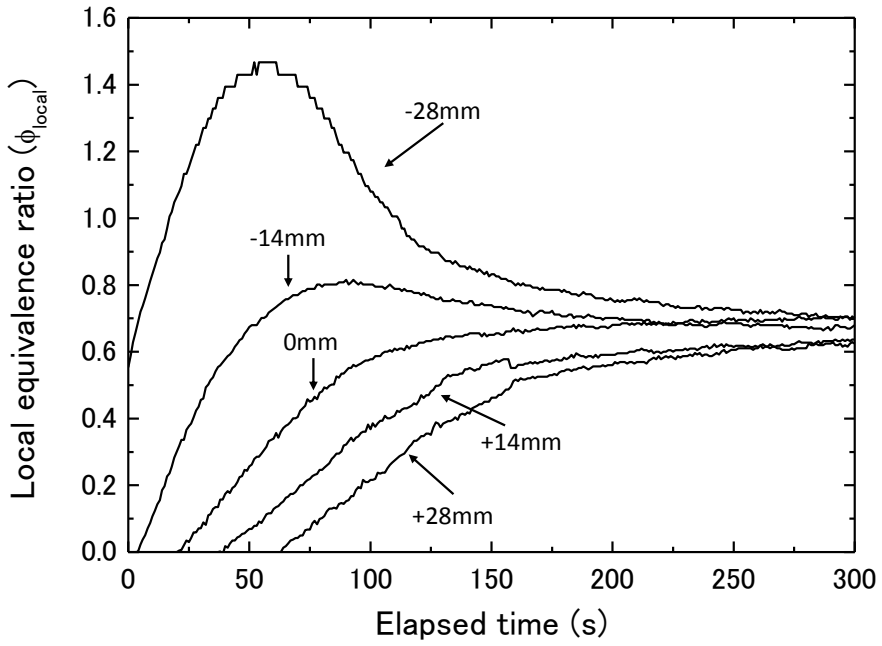

Figure 3.8 Growth of equivalence ratio at various location inside the cylinder. The pressure is 0.101MPa, and the ambience temperature was 298K.

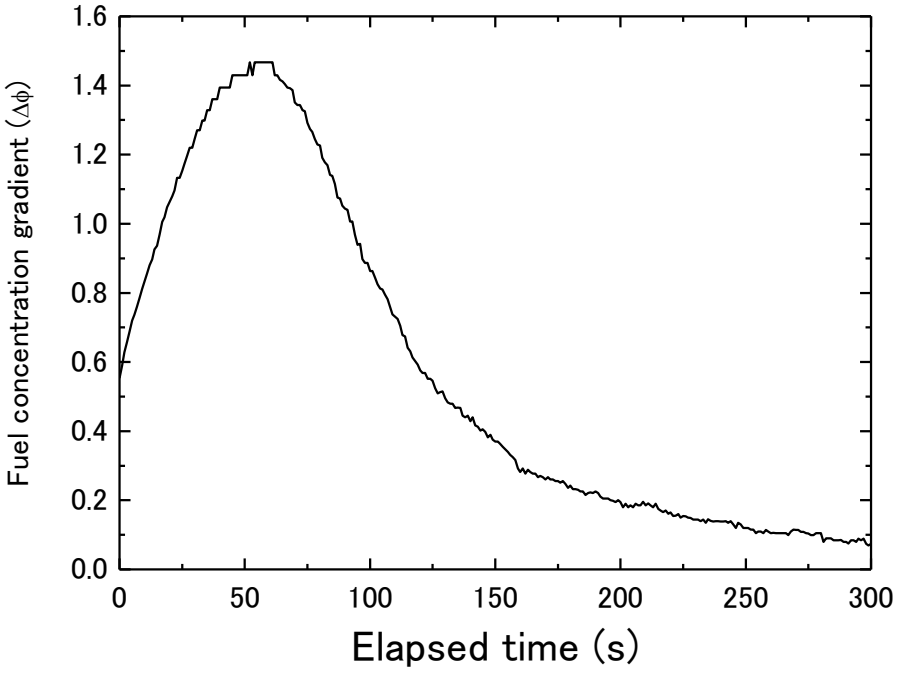

Figure 3.9 Change of ΔØ of the fuel concentration gradient (FCG) inside the cylinder. The pressure is 0.101MPa, and the ambience temperature was 298K.

In measuring FCG in model cylinder, air-CO_2 mixture gas was first introduced inside cylinder at 0.101MPa pressure. After that, fuel was carefully injected from the bottom part of the model cylinder and then let the fuel to evaporate naturally for a certain calculated time. As fuel started to evaporate upwards, the bottom part had richer Ø compared with the upper part of the cylinder. As shown again in Figure 3.7, a parameter ΔØ of FCG is defined as the difference between the highest fuel ER. Highest ER normally recorded at the lowest point of cylinder (z=-28) and the lowest equivalence ratio, usually recorded at the highest point (z=+28), thus $\Delta Ø = Ø_{-28} - Ø_{+28}$. For example, if $Ø_{local}$ at z=+28 mm and z=-28 mm are 0.1 and 1.1 respectively, then the ΔØ is 1.0.

Result for measuring FCG, obtained local equivalence ratio vs. the waiting time at total equivalence ratio of 0.6 is shown in Figure 3.8, and corresponding ΔØ is shown in Figure 3.9. Measurement of $Ø_{local}$ at each observation point conducted three times and mean value $Ø_{local}$ plotted in Figure 3.8. Therefore, accuracy of value FCG and reproducibility of equivalence ratio profiles at each observation point could be achieved. Note that at the lowest point in the cylinder (z=-28 mm), the equivalence ratio increased at a large rate for the first 50 s and reach peak at about 60 s. With further elapsed time, $Ø_{local}$ at this point decreased until 100 s. On the other hand, at uppermost region (z=28 mm), $Ø_{local}$ start to increase after 60 s and then increased with slow rate until 300 s. At 300 s, all $Ø_{local}$s almost converged at 0.6, and ΔØ becomes a very low value, 0.074. The value of ΔØ showed the peak at approximately 60s, which was about 1.47. With FCG applied in combustion chamber, the equivalence ratio is different at each point, and the specific heat ratio is also different. Therefore, during the adiabatic compression process in RCM, it is expected that the larger ΔØ is applied, the larger temperature gradient exists. Thereby, the higher temperature is at the top side of the chamber, and lower temperature is on the opposite side. The developed infrared emission temperature measurement system in this study could measure the temperature distribution in the range from 650K-1100K, was used. Auto-ignition experiments with various degree of ΔØ by changing the waiting time being conducted, and discussion of the effect ΔØ on the temperature profile and knock intensity can be found in later chapter.

3.4 Explanation about Pressure profiles and Knock Intensity

As shown in Figure 3.1, a pressure probe installed inside combustion chamber for measuring pressure changes inside cylinder once compression process begin. An example of pressure traces recorded during auto-ignition process shown in Figure 3.10.

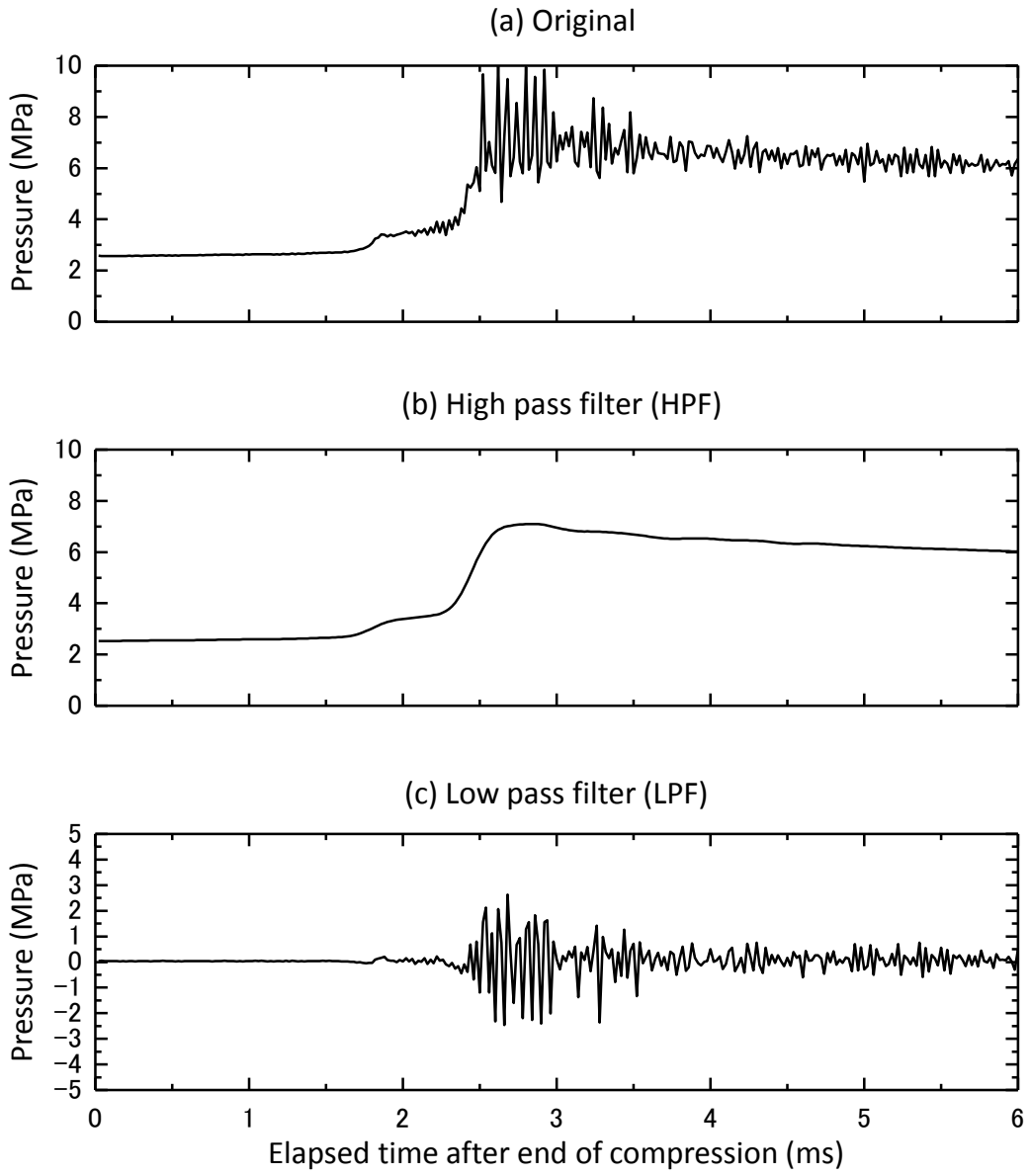

Figure 3.10 Pressure profiles recorded in cylinder and then being filtered into high and low pass filter. The initial pressure is 0.101MPa, initial temperature is 298K and compression ratio is 11. A small amount of CO_2 (4%vol) was doped prior compression begin.

Changes in pressure recorded right after compression process begin in RCM. However, auto-ignition process will begin after gas mixture being compressed at high pressure. Therefore, it is convenient to compile pressure trace depend on compression completed for further analysis. Figure 3.10 (a) shows pressure profile in cylinder during auto-ignition process occurred. An equivalence ratio of ϕ=0.5 was applied here and so called two-stage ignition successfully being presented in this figure. In this experiment, knock was observed occurred based on noticeable pressure oscillation during combustion process. This pressure trace data then being filtered into high and low pass filter for further analysis and can be referred in Figure 3.10 (b) & (c).

Low pass filter (LPF) graph Figure 3.10 (b) is useful to monitor several effect such as ignition delays, heat release rate (dP/dt) and also maximum pressure achieved. On the other hand, plot data in high pass filter (HPF) showed in Figure 3.10(c) can be use in evaluating knock intensity.

4. Temperature Distribution Measurement during Low Temperature Reaction in Auto-ignition Process

4.1 Introduction

This chapter will discuss assessment of experiment setup for measuring temperature development behavior for auto-ignition process in rapid compression machine simulating a HCCI engine. In the experiments, n-heptane was used as the fuel, and the charge mixture was compressed in homogeneous manner with varying compression ratio. Infrared emission method was used to capture the temperature distribution, and CO_2 gas was used as the emission medium, as CO_2 has strong emission band near 4.3 – 4.5 μm. The emitted radiation was recorded by a high-speed infrared camera. The relationship between the emitted energy and the medium temperature was calculated with RADCAL code, and the database for different pressures and temperatures within relevant ranges to engine combustion was prepared in advance. The obtained results show that the temperatures in

the cylinder were not uniform due to a roll-up vortex right after the compression. The difference in the temperature distribution behavior at different equivalence ratio during the ignition delay was successfully captured. The developed technique could be applied for detecting the slight temperature change due the low temperature reaction and the motion of the charge.

4.2 Effect of doping carbon dioxide (CO_2) in combustion phase

As mentioned in previous chapter, about 4% (by volume) of carbon dioxide gas (CO_2) was doped in combustion chamber prior compression process begin. By comparing with the fact that is only 0.0397%(vol) of CO_2 exist in normal air, amount of doped CO_2 is quite significant. Although CO_2 are one of major products in hydrocarbon combustion, it is necessary to study effect of doping such amount of CO_2 into combustion phase. In this chapter, we attempt to measure the effect of this CO_2 gas more in physical manner, however little explanation in chemical reaction also will be discussed.

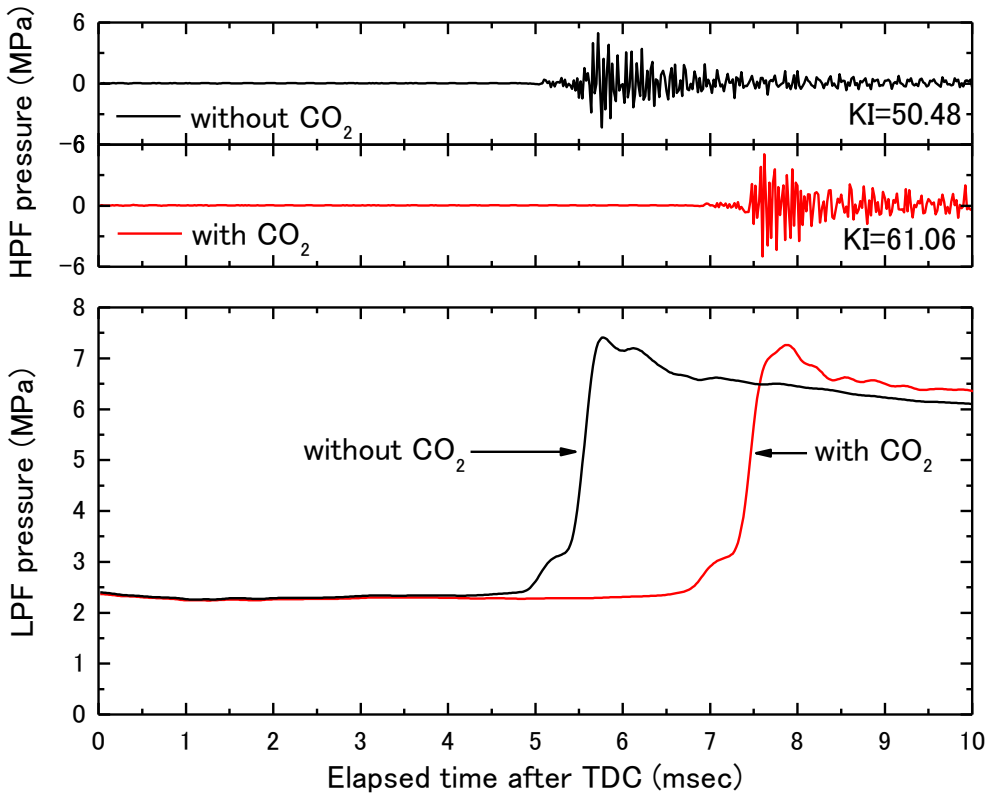

Figure 4.1 Effect of doping CO_2 (4%vol) in cylinder on homogeneous combustion process using n-heptane as fuel. Experiment condition; Pi=0.101MPa, Ti=298K and φ=0.6

Figure 4.1 shows pressure profiles for experiment conducted with and without CO_2 doped in cylinder. The lower curve is the pressure through low-pass filter, and the upper graph is the pressure through high-pass filter. Experiment conducted in homogeneous manner and ER were set to be 0.6. Both of experiments successfully exhibit two-stage ignition phase. In low pass filter (LPF) graph, maximum pressure shows no great different between experiment conditions. However in the same graph, it can be observed that pressure traces shows noticeable different in ignition delay as the one with CO_2 experience longer ignition delay approximately 2 ms. Knock occurred in both experiments and can be observed with pressure oscillation in high pass filter (HPF) graph. Knock intensity shows at right side of graph indicated that experiment with CO_2 shows intensity of knock (KI) was increased about 21% compare with one without CO_2. From this figure, effect of doping CO_2 prior auto-ignition compression can be drawn as follows:

a. CO_2 have lower specific heat ratio compare with the air. Therefore, injected amount of 4% vol contributes overall specific heat of gas mixture to reduce about 0.29% than air. Consequently temperature at TDC is getting lower which then suppress lower temperature kinetics.
b. CO_2 suppress low temperature kinetics like effect of applying exhaust gas recirculation (EGR) in engine.
c. Suppression of low temperature kinetics contributes to longer ignition delay.
d. Longer ignition delay caused maximum pressure increased as well as knock intensity. This phenomenon is similar to condition auto-ignition compression that is richer ϕ affect longer ignition delay.

4.3 Temperature measurement at TDC Condition without Combustion

As in this study focus on measuring distribution temperature inside cylinder, accuracy of experiment set up need to be evaluated first. Therefore, comparison between predicted temperature and measured temperature was conducted. From known parameter of initial

temperature, initial pressure, compression ratio, specific heat of gas mixture and pressure at TDC, temperature at TDC able to be predicted. Upon compression begin until compression completed, development of temperature inside cylinder undergo chemical kinetics reaction based on two assumptions, i.e. compression complete in polytrope process (η=1.37 & 1.39) or adiabatic process. Then accuracy of the calculated temperature at TDC were checked by experiments with RCM of two different conditions i.e.:

a. air (without fuel) with CO_2 gas (4.0%vol).
b. nitrogen gas-CO_2 gas (4%vol) and n-heptane (corresponding ϕ=0.4, if the air was used) as fuel.

The other conducted with various experimental parameters were the compression ratio (CR) to be 10.0, 11.0 and 12.0. The initial pressure (Pi) set to be at 0.101MPa, and the initial temperature (Ti) to be fixed at 298K. The amount of CO_2 gas was determined so that HSIR camera could capture sufficient emission intensity at TDC condition (Kamarrudin *et al.* 2013).

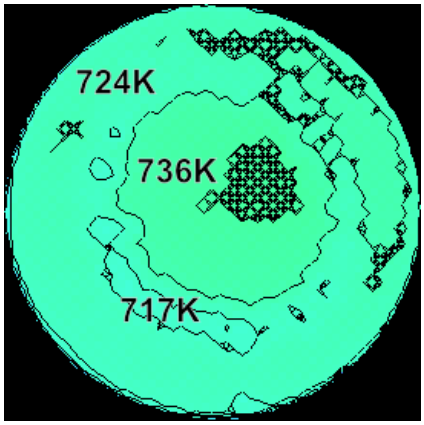

Figure 4.2 Temperature distribution inside combustion cylinder with contours every 10 K. Compression mixture: air and CO_2 (4.0%vol). Pi = 0.101MPa, Ti=298K and CR=11.0

Figure 4.2 shows the temperature distributions at TDC for CR of 11.0. Interpolation drew the contour lines with the surrounding measurement points. The charge is air including 4%vol of CO_2. No fuel was introduced in cylinder. The temperature data are converted from the emission of the medium gas captured by HSIR camera. It can be seen that there is a lower temperature ring-shape region between the center and the cylinder wall. This region is difficult to be recognized at TDC condition. However, when the temperature increases due to the low temperature reaction, this region will appear clearly as ring shape pattern that will be shown later. This ring shape is known as a roll-up vortex. Roll-up vortex was presence due effect of mixing cold gas from boundary layer with hot gas in the core region. Depending on the experiment parameters, the temperature inside roll-up vortex usually recorded to be up to 30K lower compared with the surroundings. For the case of initial temperature, Ti, was 298K, the calculated polytropic and adiabatic temperature in the cylinder was 732K and 755K respectively. The polytropic index was calculated from pressure history and the compression ratio. The measured temperature was distributed from 724.7K to 741.7K, and the core temperature, which is 736K, is between the adiabatic and polytropic temperatures.

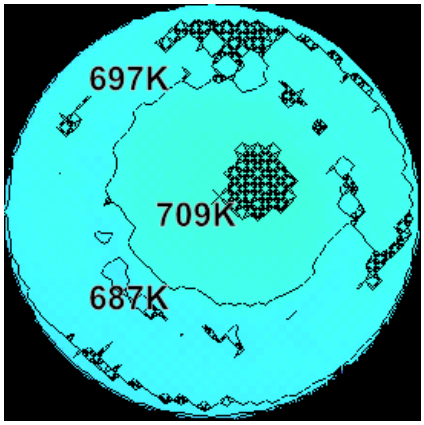

Figure 4.3 Temperature distribution inside combustion cylinder with contours every 10 K. Compression mixture : nitrogen, CO_2 (4.0%vol) and n-heptane (ϕ=0.4). Pi=0.101MPa, Ti = 298K and CR=11.0

The TDC temperature for nitrogen and n-heptane mixture (ϕ =0.4) including 4%vol CO_2 are shown in Figure 4.3. The CR is 11.0. The calculated polytropic and adiabatic temperatures were 699K and 730K respectively. The measured temperature inside the cylinder shows the temperature distribution in the range from 697.9K to 711.0K. Based on the above mentioned data, it is found that these experimental values agreed well with the estimated temperature from the pressure data.

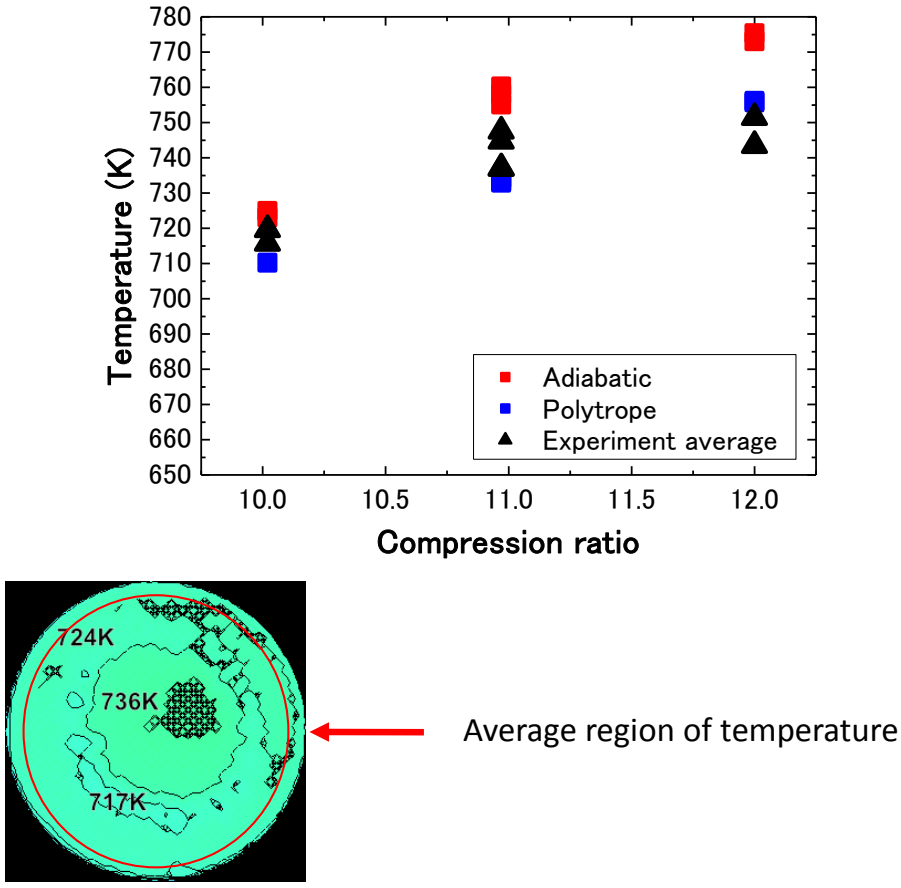

Figure 4.4 Comparison between experimental data and calculated temperature at TDC for adiabatic and polytropic processes with three different CRs. The charge was Air-CO_2 (4%vol)

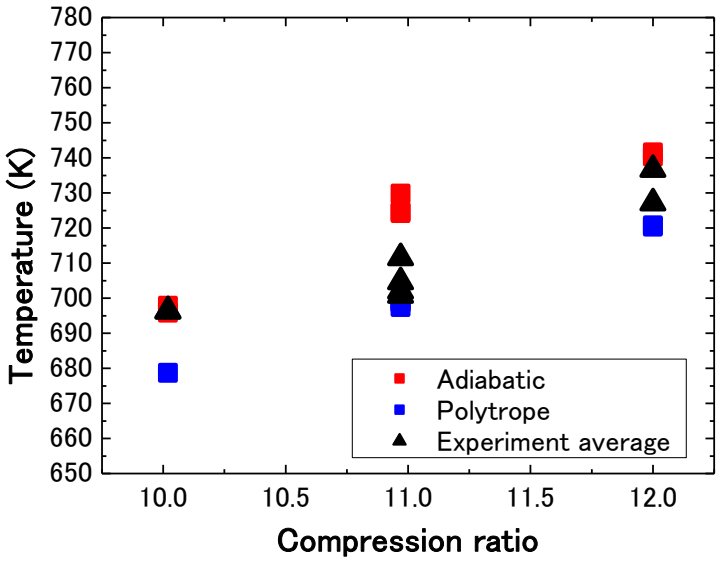

Figure 4.5 Comparison between experimental data and calculated temperature at TDC for adiabatic and polytropic processes with three different CRs. The charge was N_2-CO_2 (4%vol)-n-heptane (ϕ: 0.4)

Other obtained temperature at TDC, (T_{TDC}) with various compression ratio, with and without fuel cases were plotted in Figure 4.4 and Figure 4.5. The average temperatures in the graphs refer to the temperature within red ring in below of Figure 4.4. These average temperature are plotted for comparison with the adiabatic temperature and the polytropic temperature calculated from the pressure history. The adiabatic process takes account of the temperature dependence of the ratio of specific heats. In Figure 4.4, T_{TDC} increases with CR monotonically. The maximum T_{TDC} for CR=10.0 is slightly over than adiabatic process, whereas the maximum T_{TDC} for CR=12.0 recorded lower value than the polytropic temperature. Although the results contain such errors, the obtained temperature was reasonable because the maximum temperature was between the adiabatic temperature and the polytropic temperature.

For gas mixture that includes fuel, nitrogen gas that have similar specific heat ratio with air was used as the inert gas instead of air. The step is necessary for avoiding chemical reaction during the compression. In Figure 4.5, the effect of low specific heat ratio of n-heptane are obvious; which can be observed that the T_{TDC} is significantly lower about 30K-40K. For fuel-N_2 mixture, the accuracy of the obtained temperature is also reasonable.

4.4 Temperature Measurement within Ignition Delay

Once accuracy at TDC was tested, next stage is to check whether experiment set up is capable to measure temperature growth in cylinder and how far of its accuracy. In this chapter, author carried out the experiments with three different equivalence ratio (ϕ), i.e. 0.3, 0.5 and 0.6. The initial pressure is 0.101MPa, and the CR is 11.0, with the initial temperature is 298K. The pressure profiles for these experiments were shown in Figure 4.6. The well-used definition adopted here that the ignition delay from TDC till the cool flame appears denoted as $\tau 1$. The ignition delay after $\tau 1$ until the thermal flame appears denoted as $\tau 2$, which shown at the upper graph in Figure 4.6.

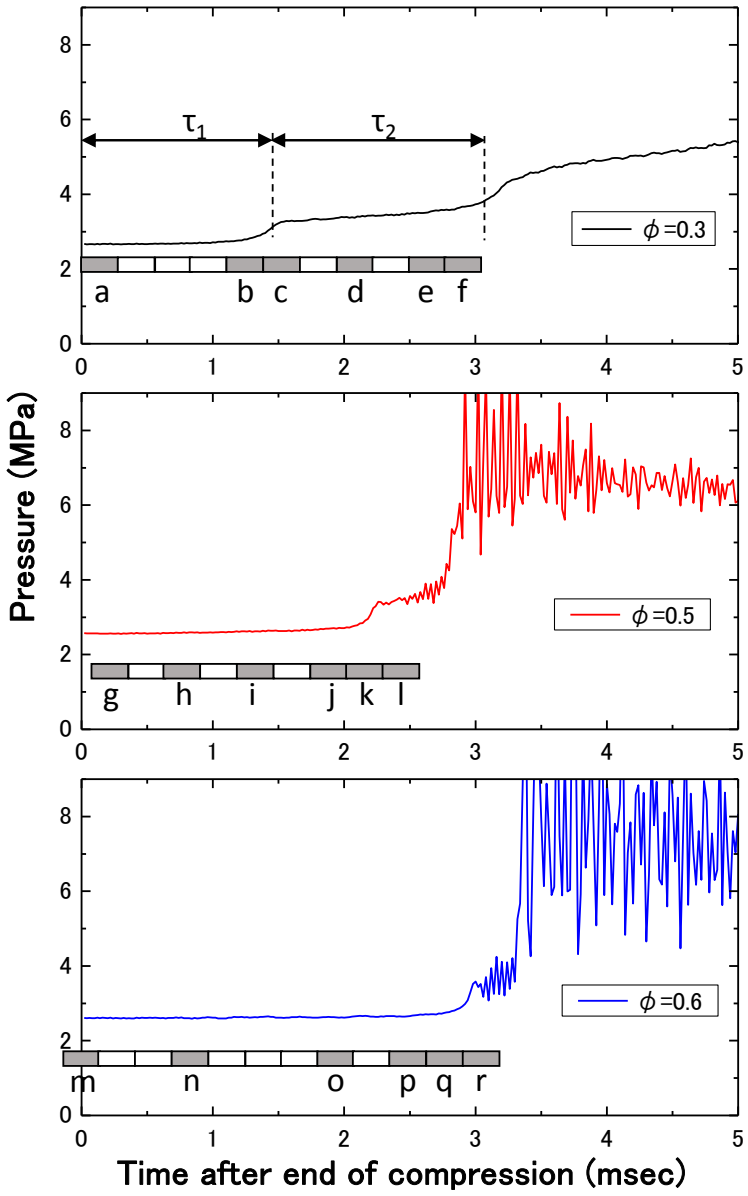

Figure 4.6 Pressure histories at ϕ=0.3, 0.5 and 0.6 of n-heptane-air-CO_2 mixture in RCM. Pi=0.101MPa, Ti was set approximately 298K. The compression ratio was 11.0.

For a leaner ϕ of 0.3, so-called two-stage ignitions occurred and it could be seen from two times increment of the pressure trace. Almost no pressure oscillation was observed,

and therefore knocking does not occur in this condition. For the richer condition, (ϕ=0.6), two-stage ignition was still able to observe however it is hard to distinguish between first and second stages. Combustion process complete in almost single ignition (accompanied with very short second ignition delay), with heavy knock intensity comparing with other experiments. The τ_1 was shortest for ϕ=0.3, and was longest for ϕ=0.6. On the other hand, the τ_2 has opposed trend to τ_1. This is a well-known trend in the NTC region (Curran *et al.* 1998), and it is thought that the observed result comes from the difference in the equivalence ratio and the temperature at TDC due to the difference in the specific heat ratio.

Figure 4.7 shows the temperature distribution inside the cylinder after TDC, which corresponded to the experiments shown in Figure 4.6. The indexes (a) – (r) in correspond to the frame bar labeled in Figure 4.6. The results are shown here agreed with our previous study that the temperature distribution right after TDC does exist, which is caused by the movement of the piston during the compression process. Furthermore, a roll up vortex phenomenon becomes clear as the temperature increase.

For lower ϕ, the T_{TDC} of the mixture should have higher value because it has higher specific heat ratio. Figure 4.7 shows the consistent results; T_{TDC}=726K for ϕ=0.3 (Figure 4.7a), T_{TDC}=714K for ϕ=0.5 (Figure 4.7g), and T_{TDC}=704K for ϕ=0.6 (Figure 4.7m), respectively. The results are consistent with the theoretical anticipation.

ϕ=0.3

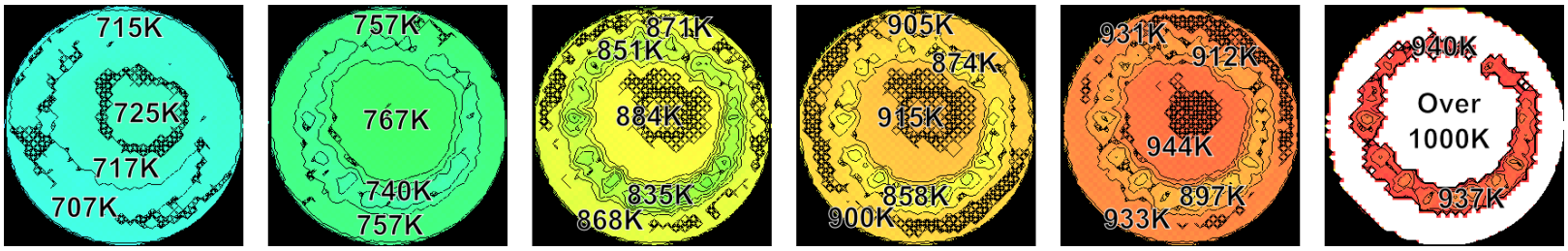

(a) -0.02 - 0.24ms T_{core}=726 K

(b) 1.09 - 1.35ms T_{core}=761 K

(c) 1.37 - 1.63ms T_{core}=858 K

(d)1.93 - 2.19ms T_{core}=922 K

(e) 2.48 - 2.74ms T_{core}=958 K

(f) 2.76 - 3.02ms T_{core}=993 K

ϕ=0.5

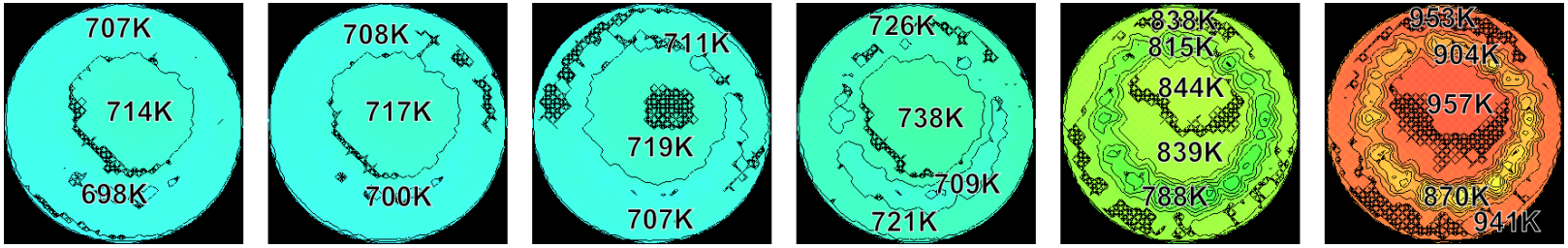

(g) 0.05 - 0.31ms T_{core}=714 K

(h) 0.60 - 0.86ms T_{core}=719 K

(i) 1.16 - 1.42ms T_{core}=730 K

(j)1.72 - 1.98ms T_{core}=748 K

(k) 1.99 - 2.25ms T_{core}=816 K

(l) 2.27 - 2.53ms T_{core}=956 K

ϕ=0.6

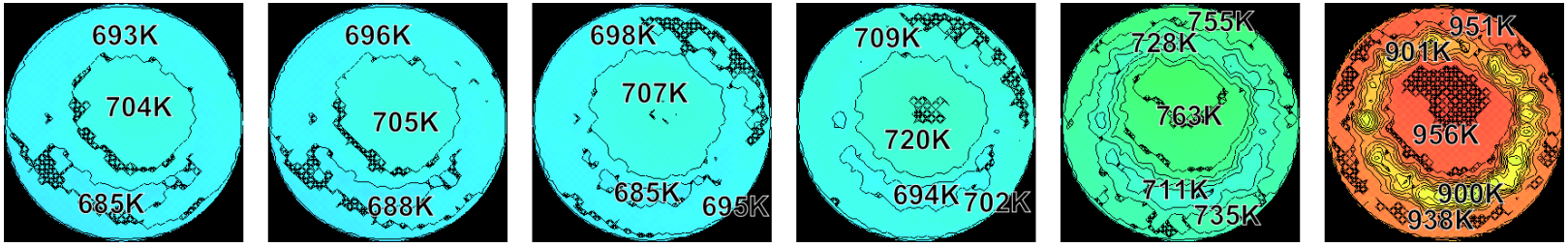

(m) -0.13- 0.13ms T_{core}=704 K

(n) 0.70 - 0.96ms T_{core}=705 K

(o) 1.81 - 2.07ms T_{core}=710 K

(p) 2.37 - 2.63ms T_{core}=721 K

(q) 2.65 - 2.91ms T_{core}=748 K

(r) 2.92 - 3.18ms T_{core}=927 K

Figure 4.7 Temperature distribution obtained with infrared emission method with contours every 10 K. ϕ=0.3, 0.5 and 0.6. Pi=0.101MPa, and Ti was set approximately 298K.

As shown in Figure 4.6, there occurred two-stage ignition for ϕ=0.3 and 0.5. Then the temperature during low temperature reaction in these cases was being verified. The pressure in the cylinder for ϕ=0.3 increased from 2.67Mpa to 2.80 MPa at t=1.35 ms, increased to 3.39 MPa at 2.19 ms and then gradually increased to 3.52 MPa till 2.74 ms as shown in Figure 4.6. Assuming the process within constant volume, the calculated temperatures at 1.35 ms, 2.19 ms and 2.74 ms are 761 K, 922 K and 958 K, respectively, if the initial core temperature was assumed as 726 K as shown in Figure 4.7 (a). The corresponding measured temperature within τ_1 period increased from 726 K to 767K at t=1.35 ms, and increased to 915 K at 2.19 ms, and finally reached 944 K at 2.74 ms. The estimated core temperature (T_{core}) at each frame is shown in Figure 4.7. T_{core} was defined as temperature located near the center of the cylinder so that effect of roll up vortex and the heat loss to the side wall were assumed to be negligible. In this experiment, T_{core} was defined to be within 20mm in diameter size from center of cylinder. The T_{core} at TDC (refer Figure 4.7(a),(g) & (m), were the temperature that was obtained by the emission method developed. Therefore, the absolute value may contain some error. The rest core temperatures after TDC in Figure 4.7 were calculated based on pressure history with the assumption that the volume kept constant. Thus, the obtained core temperatures agreed with the estimation quantitatively, and also the results give information of temperature distributions.

As shown in Figure 4.7 (f), it is found that there is white region inside of cylinder that indicates over 1000 K. According to the pressure history in Figure 4.6, the thermal flame begins to appear at the moment. Therefore, in Figure 4.7(f), huge radiation is released, and additionally the amount of CO_2 increases as combustion products. As the amount of CO_2 increased to some unknown value than the initial concentration, the temperature at this time onwards is out of the target of this study.

For ϕ=0.5, after the relatively long τ_1 period, the pressure increased from 2.56 MPa to 3.44 MPa, and after a short time the rapid pressure rise due to the thermal flame appeared. The estimated temperature during τ_2 is 956 K, and the temperature in Figure 4.7 (l) is 957 K, which agrees with the estimation.

For ϕ=0.6, longer τ_1 period is observed due to low T_{TDC}. The temperature during τ_1 period is almost the same till t=2.63 ms. After that the temperature slightly increased due to the beginning of low temperature reaction (Figure 4.7(q)), then the thermal flame follows after very short τ_2.

In all conditions, the obtained temperature and the calculated core temperature were consistent, and the infrared emission method could distinguish the temperature difference about 10K in the cylinder. However, when the pressure change was rapid or pressure oscillation occurred during the exposure time, such as Figure 4.7(c), (k) and (r), the difference between the core temperature and the obtained temperature became large. The rapid change of temperature during the camera exposure time could cause reasonable error in the calculated temperature.

4.5 Conclusion

An experimental study was conducted to measure the temporal temperature distribution in RCM by applying the infrared emission method with 4.3 μm band of carbon dioxide. As the results, the followings are concluded.

1. The temperature of the no-reacting charge with varying the compression ratio and that adding the fuel agreed with the theoretical estimation. The developed temperature measurement technique could distinguish the temperature difference about 10 K. Additionally the characteristics temperature distribution due to the movement of the piston called a roll up vortex was successfully captured. The results showed that temperature at roll up vortex region was 10-30 K lower than the core temperature.

2. The temporal behavior of the temperature profile of the reacting charge in the cylinder during the ignition delay was successfully captured. Not only the temperature change due to the appearance of cool flame but also the gradual temperature increasing during the low temperature reaction were captured quantitatively as two-dimensional information. Such information is useful for interpret the auto-ignition phenomena of the compressed charge.

5. Behavior of Temperature Profile during Low Temperature Oxidation of Auto-ignition Process with Fuel Concentration Gradient

5.1 Introduction

An experimental study was conducted to investigate the patterns of the temperature distribution in a rapid compression machine, inside the cylinder during the auto-ignition process, with a stratified fuel distribution. The fuel concentration gradient (FCG) was created by injecting the fuel from the bottom part of the cylinder followed by a waiting time before compression begin. The overall equivalence ratio was set to 0.6, and the compression ratio was set to 10. The relation between the difference of the equivalence ratios at the top and the bottom cylinder sides, $\Delta\emptyset$, and the waiting time from the injection, t_w, was investigated in advance. The data obtained showed that the low temperature oxidation process started to occur from the leaner $\Delta\emptyset$ region. On the other hand, the ignition location of hot flame depend on magnitude of $\Delta\emptyset$ applied in cylinder. The knock

intensity (KI) could be weakened when a proper FCG is applied, but in the cases where the FCG is too steep or inadequate, lower combustion efficiency or a large KI would respectively occur.

5.2 Effect of Applying Fuel Concentration Gradient in Gas Charge

First, we checked the FCG at TDC. Figure 5.1 shows the temperature distribution in cylinder with various FCG. It was found that the temperature at bottom part (leaner Ø) of the cylinder was lower than that at the upper part (richer Ø) of the cylinder. The larger ΔØ is, the larger the temperature difference becomes. When ΔØ was more than 1, it was observed that the horizontal layers of temperature existed. However, the temperature at the center part of the cylinder recorded the highest value in almost cases. The reason might be that the center part was far from the cylinder wall which usually had colder temperature and additionally there might be mixing effect due to the roll up vortex. In Figure 5.1, the temperature difference was too small to recognize FCG clearly. Hence, we focus the temperature at the center of the cylinder.

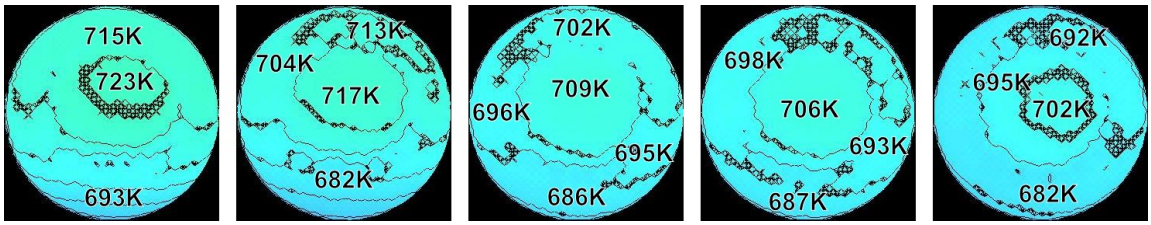

a) tw=60s, Δ∅=1.467 b) tw=100s, Δ∅=0.863 c) tw=170s, Δ∅=0.260 d) tw=210s, Δ∅=0.185 e) tw=300s, Δ∅=0.074

Figure 5.1 Temperature distribution s inside the cylinder at TDC with various FCG.

As shown in Figure 3.8, the development of local equivalence ratio at z=0 mm, $Ø_0$, increased significantly from 0 s until about 125 s, after that the growth rate of $Ø_0$ became slow This temporal change of $Ø_0$ was observed as the change of temperature profiles in center region in Figure 5.1, in which the temperature of the center part increased with the waiting time from the fuel injection, that is, the center temperature at 60 s was 723K, and it decreased to 717 K at 100 s, then converged to 702 K after that. Of course, there was some mixing effect of roll up vortex as shown in our previous research, but we assumed there existed a proper FCG, which was proportional to the initial FCG before compression.

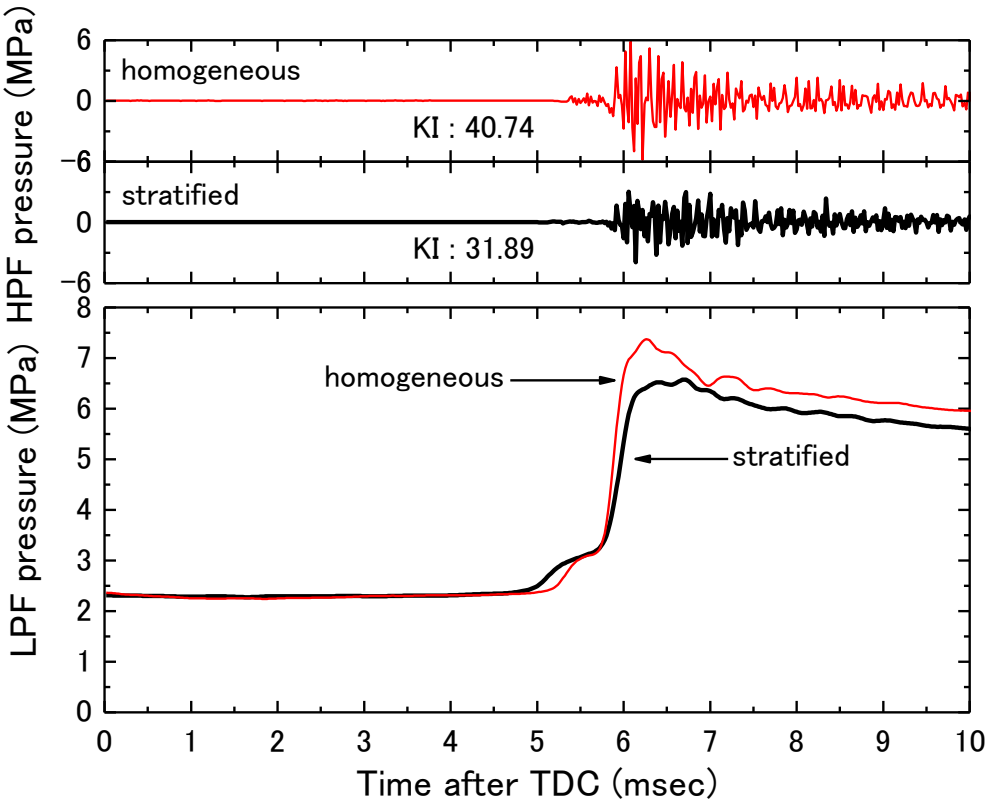

Figure 5.2 Pressure history during auto-ignition process of homogeneous charge and stratified charge of Δ⌀=0.074.

Figure 5.2 shows the pressure history during the auto-ignition process with homogeneous and stratified mixture, respectively. The total equivalence ratio was 0.6, and ΔØ was 0.074, which corresponded to the waiting time of 300 s. The recorded pressure profiles was filtered with low pass filter (lower graph) and high pass filter (upper graph), respectively. The cut off frequency was 5kHz. The applied ΔØ was very small, therefore, the low pass filtered (LPF) pressure histories are not different so much except that the second induction time (τ_2) of stratified charge was a little longer. In these histories, clear two-stage ignition was observed. However, the knock intensity was much reduced by the small ΔØ. The knock intensity (KI) was calculated from the high pass filtered (HPF) pressure history with the definition by Konig et al [6].

$$KI = \frac{1}{N}\sum_{i=1}^{N}(p_i' - p'_{mean}) \quad (1)$$

where the N is the total sampling number during knocking, and the i is the sequential number of pressure data obtained. The sampling frequency was 50kHz. By referring HPF graphs in Figure 5.2, the duration of the knocking was determined as the time between the start when the HPF pressure exceed 2% of maximum pressure (P_{max}) in both positive and negative value, and the end where the pressure oscillation became less than 2% of the maximum pressure in LPF pressure history.

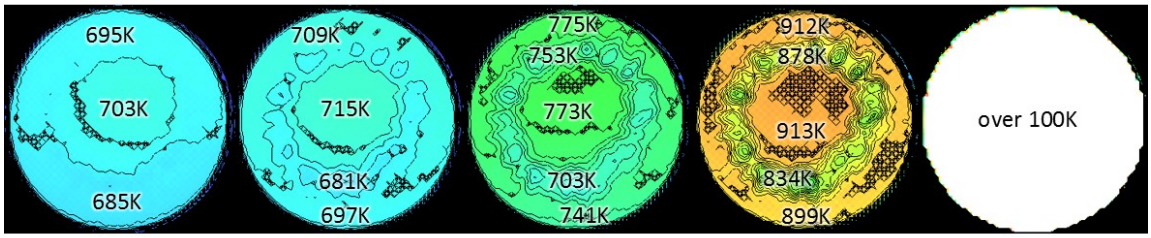

t = 0.00 ms (TDC) t=5.28 ms t = 5.56 ms t = 5.84 ms t = 6.11 ms

a) homogeneous charge

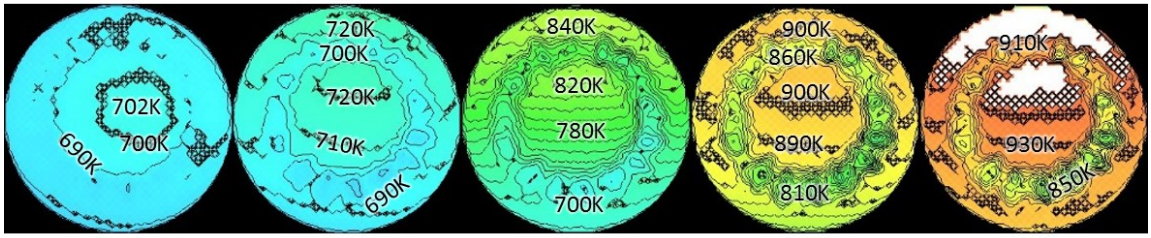

t = 0.00 ms (TDC) t=5.28 ms t = 5.56 ms t = 5.84 ms t = 6.11 ms

b) stratified charge

Figure 5.3 Temperature distributions inside the cylinder during auto-ignition process in a) homogeneous charge and b) stratified charge of ΔØ=0.074.

The calculated KIs were 40.74 and 31.89 for the homogeneous charge and the stratified charge, respectively, that is, the ΔØ of 0.074 reduced the KI about 22%. The difference was caused by the temperature gradient in the stratified charge during the low temperature oxidation. Figure 5.3 shows the temperature distribution after TDC till the appearance of hot flame for each case. From right after the TDC till 5.00 ms, the temperature was slightly increasing, but almost uniform except the ring-shaped lower temperature region due to roll-up vortex [4, 7]. Then, the temperature increase due to the heat release of low temperature oxidation was observed after that hot flame covered the entire cylinder. With the stratified charge, the temperature distribution after the TDC looked similar to that with the homogeneous charge; however, the obvious layered temperature distribution was observed at 5.56 ms. In the case of the above stratified charge, the equivalence ratios of leaner Ø and the richer Ø were estimated at 0.563 and 0.637, respectively. Therefore, the initial temperature distribution at TDC due to the difference

of the ratio of specific heats was not so large. But it caused the stepped low temperature oxidation shown in Figure 5.3b at t=5.56 ms, and it was found that the layered temperature distribution remained at the onset of hot flame at t=6.11 ms. This magnified temperature difference caused stepped occurrence of hot flame and reduced the magnitude of dP/dt in LPF pressure history, which resulted in reduction of the knock intensity. It was found that the hot flame started from the leaner ∅ and moved to the richer ∅, but the ring-shaped roll-up vortex region remained as shown in Figure 5.3 (b) at t=6.11 ms. It implied that the movement of the hot flame was not propagation, but the succession of auto-ignition phenomena.

5.3 Behavior of Low Temperature Oxidation and Thermal Flame in Various Fuel Concentration Gradient

Based on the above experiment, applying FCG in cylinder affected the ignition delays for both first stage and second stage of ignition, which might provide a key to control ignition timing in HCCI engine. Hence, we then conducted experiments with several Δ∅ of FCG to investigate the effect on knock intensity. Figure 5.4 shows the LPF pressure profiles with varying Δ∅. The total equivalence ratio (∅=0.6), the compression ratio (ε=10), initial pressure (Pi=0.101 MPa) and initial temperature (Ti=298 K) were not changed. The result shows that the higher Δ∅ is, the shorter the ignition delay became; it was because the low temperature oxidation process took place earlier with higher Δ∅. For example, when the Δ∅ was larger than 0.4, the ignition delay of the first stage became less than 3 ms. When the waiting time was 210 s or less, it was found that the pressure rise during the low temperature oxidation became gradual whereas it was stepwise at larger waiting time. It implied that the stratified auto-ignition occurred at larger Δ∅ conditions. On the other hand, by referring to LPF pressure profile, the maximum pressures with large Δ∅ decreased, which were less than 6 MPa. From the results shown in Figure 3.7, the local equivalence ratio at the upper part is less than 0.3 if the waiting time is less than 120 s. It is thought that the combustion efficiency drastically decreased if the mixture's equivalence ratio was less than 0.3 [8]. Therefore, when Δ∅ was more than 0.576 (t_w≦120 s), it was thought that

the combustion efficiency was insufficient due to too lean mixture at upper region of the cylinder.

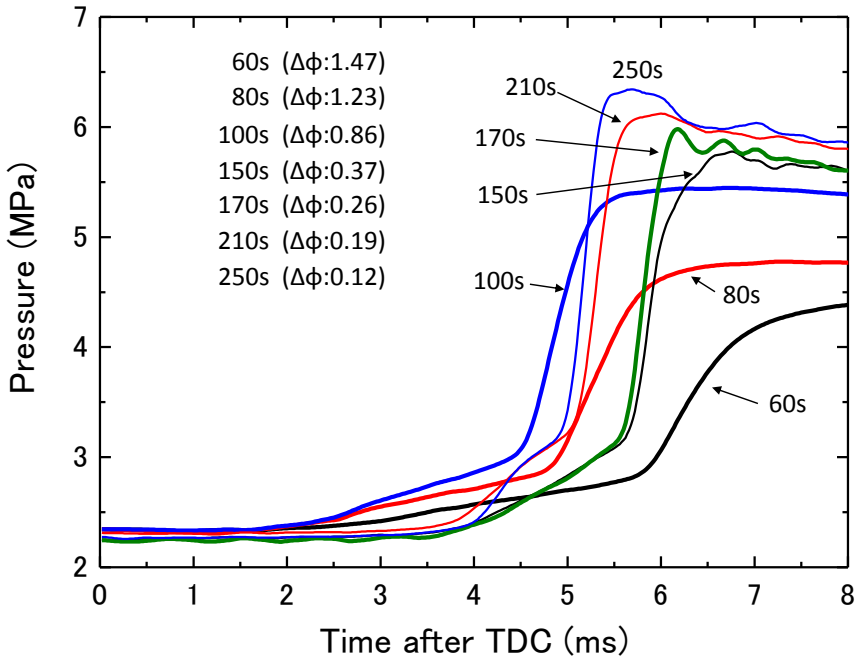

Figure 5.4 Pressure history during auto-ignition process of various FCG. Pi was 0.101MPa, Ti was 298K while φglobal was 0.6.

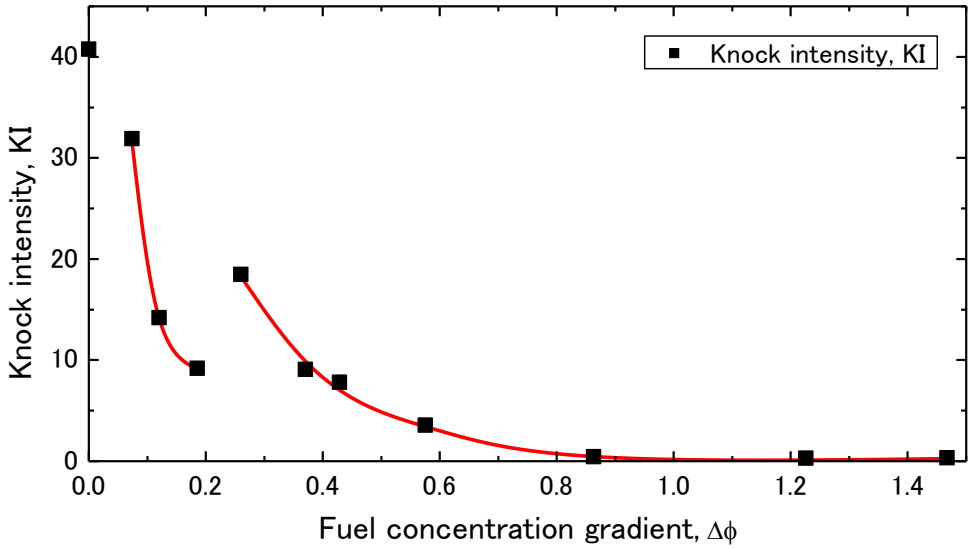

Figure 5.5 Knock intensity, KI, with varying Δ⌀ calculated from high-pass filtered pressure history

Figure 5.5 shows KI with varying ΔØ calculated from HPF pressure history. From the results, the stratified charge with higher ΔØ normally had lower KI. For example, when the ΔØ increased from 0.074 to 1.47, KI decreased from 31.89 to 0.30 and the pressure oscillation became smaller. When the ΔØ was more than 0.37, the maximum pressure also decreased with the increase of ΔØ; therefore, it is thought that the reason of the reduction of KI is not only the effect of locally shifted ignition as shown in Figure 5.3 (b), but also the incomplete combustion due to locally too lean mixture. When ΔØ increased from 0.07 to 0.19, KI first decreased drastically, but interestingly that when FCG at ΔØ=0.260, KI value suddenly increased up to 18.4 and then start to decrease again as FCG keep increase. The similar phenomenon was also observed in our other research [9], in which the KI in the mixture with a certain small FCG had larger value than that in homogeneous mixture. Therefore, it was found that there was an optimal ΔØ to reduce KI.

b) t_w = 300 s, $\Delta\phi$ = 0.07

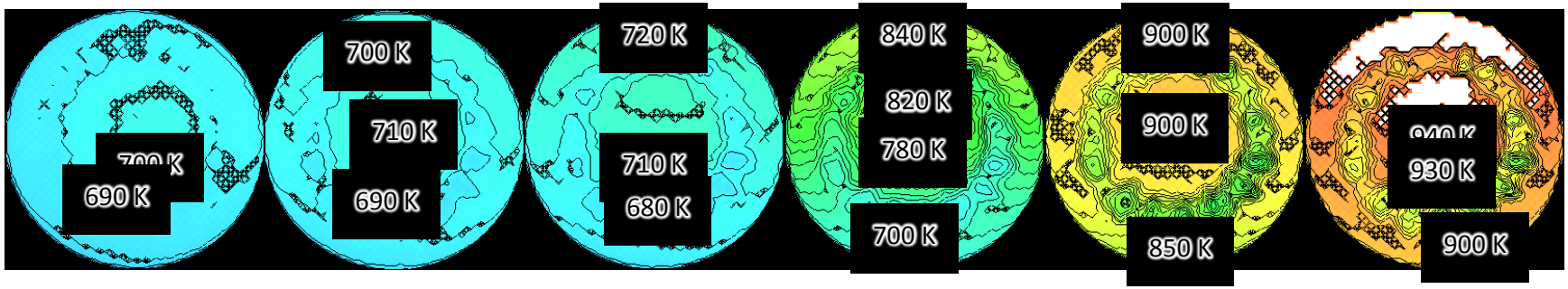

0.00 – 0.26 ms | 5.00 – 5.27 ms | 5.28 – 5.55 ms | 5.56 – 5.83 ms | 5.84 – 6.01 ms | 6.11 – 6.38 ms

c) t_w = 250 s, $\Delta\phi$ = 0.12

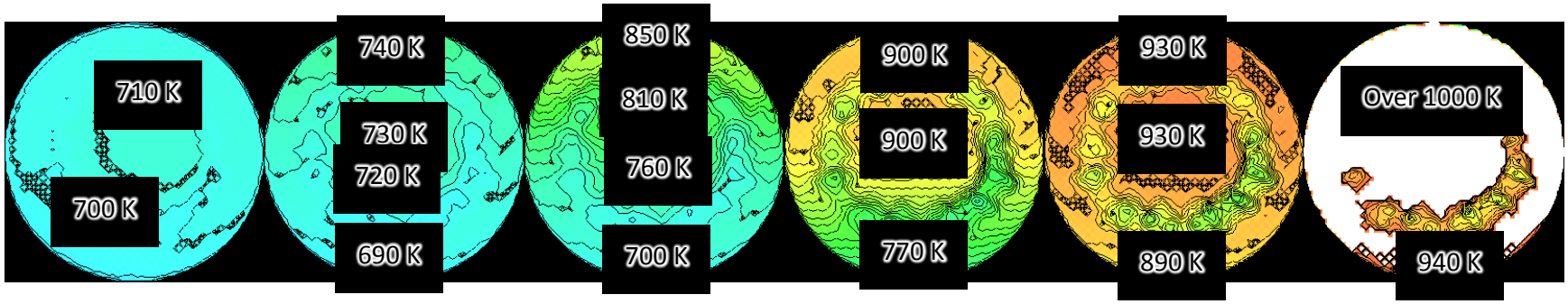

0.27 – 0.54 ms | 4.45 – 4.71 ms | 4.72 – 4.99 ms | 5.00 – 5.27 ms | 5.28 – 5.55 ms | 5.56 – 5.83ms

Figure 5.6 Temperature distributions inside the cylinder during auto-ignition process with various FCG

d) $t_w = 210$ s, $\Delta\phi = 0.19$

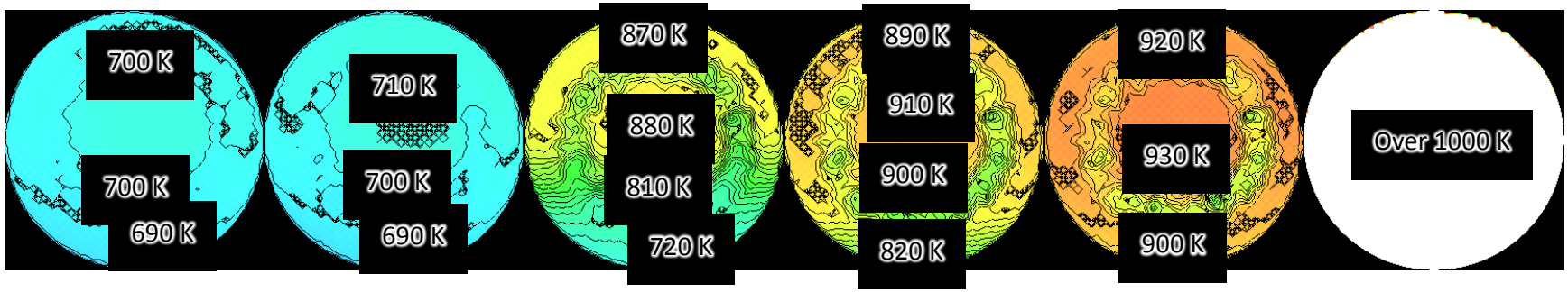

0.00 – 0.26 ms | 3.33 – 3.60 ms | 4.72 – 4.99 ms | 5.00 – 5.27 ms | 5.28 – 5.55 ms | 5.56 – 5.83 ms

e) $t_w = 170$ s, $\Delta\phi = 0.26$

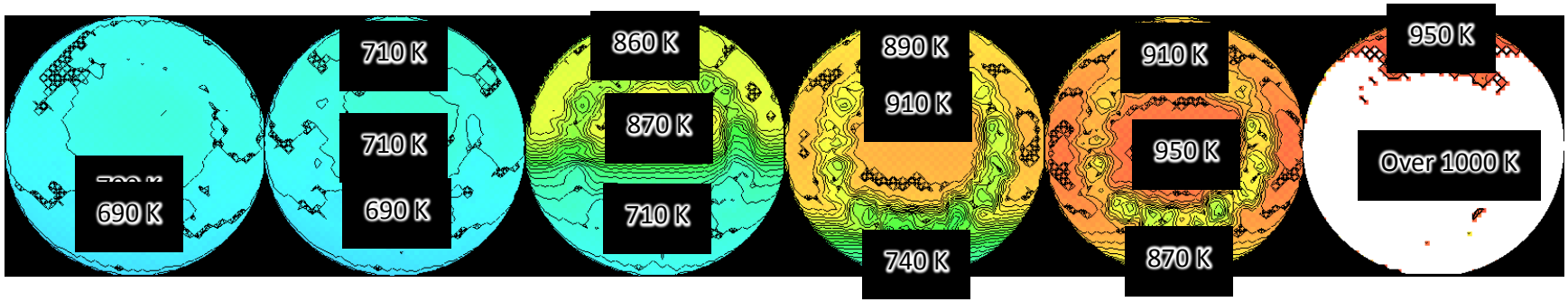

0.00 – 0.26 ms | 3.06 – 3.33 ms | 4.45 – 4.71 ms | 5.00 – 5.27 ms | 5.28 – 5.55 ms | 5.56 – 5.83 ms

Figure 5.6 Temperature distributions inside the cylinder during auto-ignition process with various FCG

f) t_w = 150 s, $\Delta\phi$ = 0.37

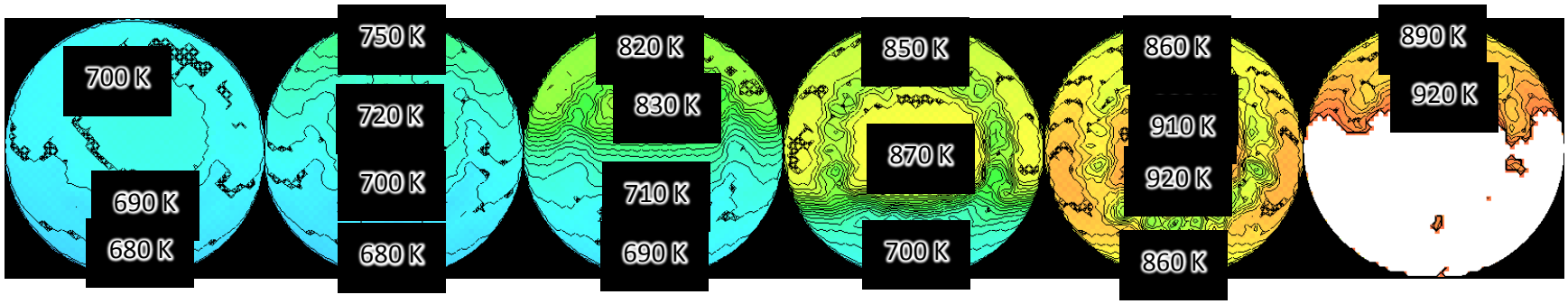

0.00 – 0.26 ms | 3.89- 4.16 ms | 4.45 – 4.71 ms | 5.00 – 5.27 ms | 5.56 – 5.83 ms | 5.84 – 6.10 ms

g) t_w = 100 s, $\Delta\phi$ = 0.86

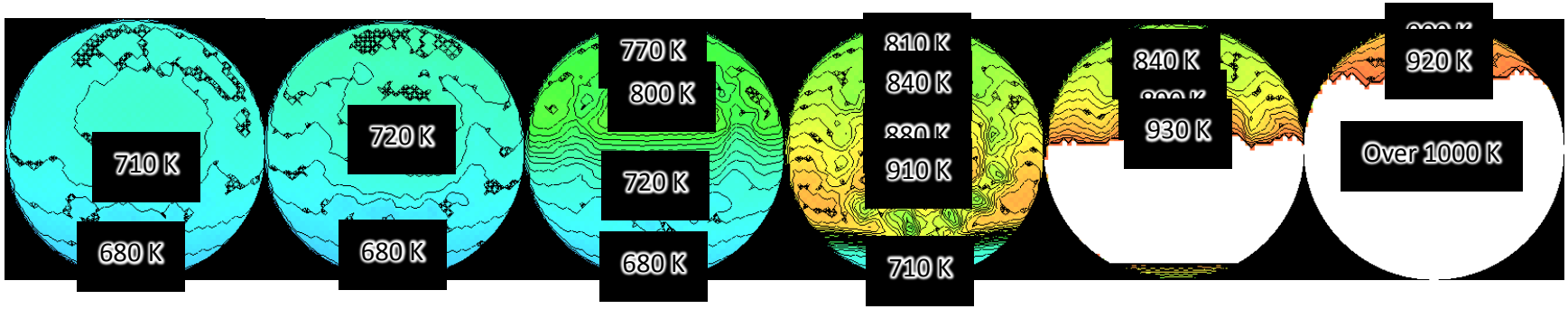

0.27 – 0.55 ms | 2.22 – 2.49 ms | 3.05 – 3.33 ms | 4.45 – 4.71 ms | 5.00 – 5.27 ms | 5.28 – 5.55 ms

Figure 5.6 Temperature distributions inside the cylinder during auto-ignition process with various FCG

h) t_w = 80 s, $\Delta\phi$ = 1.23

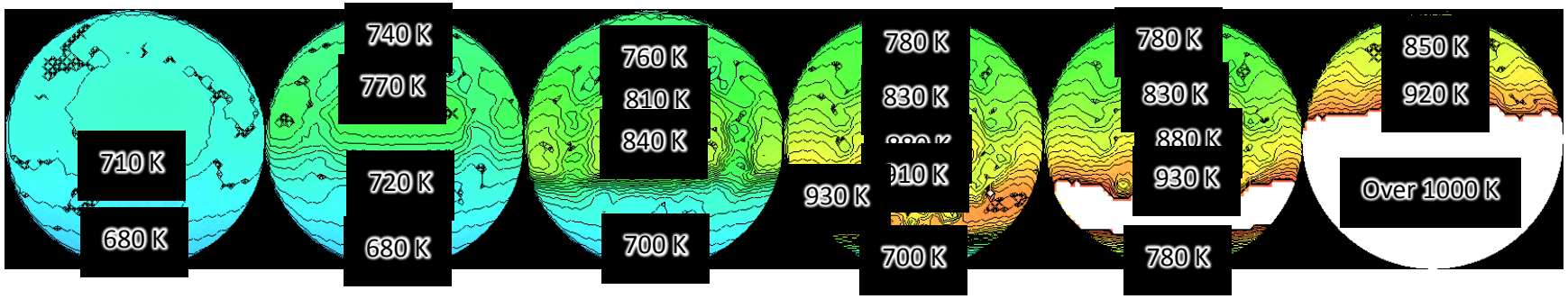

i) t_w = 60 s, $\Delta\phi$ = 1.47

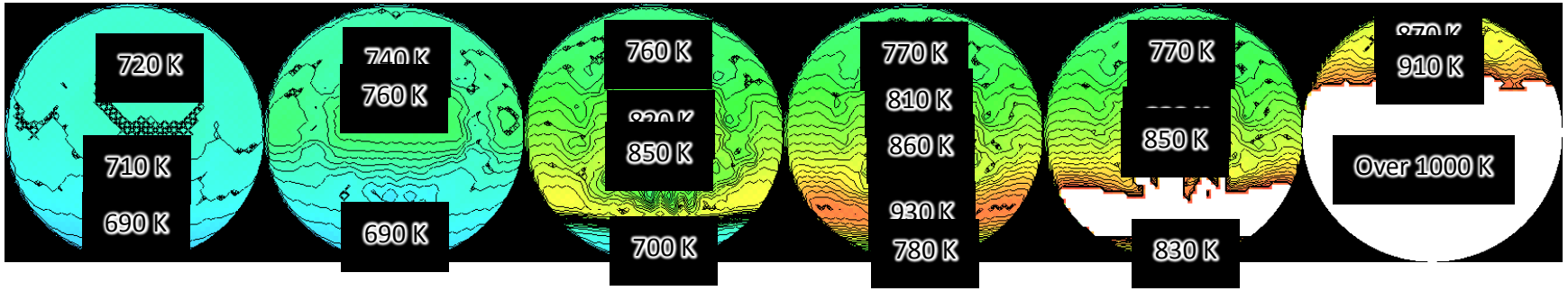

Figure 5.6 Temperature distributions inside the cylinder during auto-ignition process with various FCG

Figure 5.6 shows the temperature distribution profiles during the auto-ignition process with ΔØ of 0.12 (t_w=250 s), 0.26 (t_w=170 s), 0.37 (t_w=150 s) and 1.23 (t_w=80 s), respectively. As shown in Figure 5.4, the ignition delay of each condition was 4.45 ms, 3.89 ms, 3.78 ms and 2.78 ms, respectively. The corresponding temperature distributions are the second images of Figure 5.6 (a – d) . In all conditions, the low temperature oxidation started at the leaner Ø of the cylinder, where the temperature became higher due to the larger ratio of specific heats of leaner mixture. When ΔØ was 0.12, the cool flame moved from leaner to richer Ø and the hot flame also moved from the leaner side as similar to the case of ΔØ=0.074. On the other hand, when the ΔØ was 0.37, the hot flames started from the richer Ø side of the cylinder although the cool flame started from the leaner Ø side. The difference was caused by the low local equivalence ratio of upper side. When the waiting time was 150s, the local equivalence ratio at the upper side was about 0.45, which was near the ignition limit. In such a case, the ignition delay at the upper side became very long despite high temperature due to the lean equivalence ratio. When the waiting time was 60 s, very large ΔØ was applied to the charge. Therefore, in this case, it was expected that the local equivalence ratio in the upper region was too low to complete combustion and that in the lower part was too rich.

Figure 5.6 (d) shows that the cool flame was started at slightly upper from the center of the cylinder. As shown in Figure 5.6 (d), it was found that the local equivalence ratio at the leaner Ø was almost zero due to the too short waiting time. After the cool flame moved to the richer Ø part, the hot flame started from the boundary of the lean mixture and rich mixture, and it moved upward in contrast to the case with lower ΔØ. In the condition of ΔØ=1.23, it was obvious that the combustion efficiency was low, and this result was consistent with the lower maximum pressure in Figure 5.4. Therefore, the location where the hot flame started was different between large ΔØ and small ΔØ. When ΔØ was small, the hot flame started from the leaner Ø part as cool flame did. On the other hand, when ΔØ was large, the hot flame started at the richer Ø part although the cool flame started from the leaner side. If ΔØ has a critical value, $\Delta Ø_{,cr}$, between the two cases, it is expected that the ignition timing at each local point is close to the same value and it causes large pressure rise, which leads to large KI. In Figure 5.5, the KI at ΔØ=0.26 was 18.5, which was larger than the values of ΔØ=0.12 and ΔØ=0.37. Figure 5.6 (b) shows that the

cool flame started from the leaner Ø region, but the hot flame started from the right center of the cylinder before it cover the whole cylinder within one frame of HSIR camera. This means that, at FCG of 0.37, the leaner the mixture is, the shorter the ignition delay of cool flame, τ_1, is. However, the total ignition delay, $\tau_1+\tau_2$, is not so different in the leaner side and richer side. This leads to large heat release in a short time and the rapid combustion causes large pressure rise, dP/dt, which was the cause of large KI.

5.4 Conclusion

The effect of fuel concentration gradient (FCG) in the charge on auto-ignition process was investigated experimentally. The temperature distribution in the cylinder was measured by a high speed infrared camera with the infrared emission method. The FCG was created by injecting liquid n-heptane carefully from the bottom part of the cylinder. The following conclusion are obtained;

1. Applying FCG in the cylinder prior the compression, temperature distribution also created in the charge after the compression. The compressed charge had high temperature at the leaner Ø part and low temperature at the richer Ø part of the cylinder due to the difference in ratio of specific heats. The developed temperature measurement technique could capture the temperature profile in the compressed charge.
2. Due to the temperature distribution, cool flame started from the leaner Ø part and moved to the richer Ø part. In all conditions conducted, the cool flame started from the leaner part and the low temperature oxidation occurred in the stratified charge successively. The pressure rise due to the low temperature oxidation became gradual due to the stratified ignition delay.
3. After the stratified ignition of low temperature oxidation, relatively large temperature difference remained in the charge, and then the high temperature oxidation started. The starting point of the hot flame depended on the magnitude of ΔØ of FCG. When ΔØ was small, the hot flame moved from top to bottom as well as cool flame. When ΔØ was large, the hot flame moved

from bottom to top in contrast. There was a critical $\Delta\emptyset_{,cr}$, in which the total ignition delay at each local point became close to the same.

4. The stratified occurrence of high temperature oxidation reduced the knock intensity, KI. With increasing $\Delta\emptyset$, the KI first decreased, but then increased at $\Delta\emptyset_{,cr}$. Further increasing $\Delta\emptyset$, KI decreased again, but too large $\Delta\emptyset$ caused incomplete combustion, which resulted in low maximum pressure.

6. Numerical Study on Effect of Fuel Concentration Gradient into Low Temperature Oxidation and Thermal Flame

6.1 Introduction

Investigating on characteristics of HCCI engine not only in done experiment but also many efforts on numerical studies conducted in recent years. Almost numerical calculation conducted to focus on reducing nitrogen oxide (NOx) and particulate matter (PM) from exhaust gas. Information regarding effect on temperature distribution into the development of temperature inside cylinder was very little. Therefore, such numerical study is suggested in simple simulation model. Due to complication of calculation model, the calculating approaches can be divided into three different models, i.e. single zone model, multi zone model and multi dimension zone model. Single zone model used more on early prediction of HCCI characteristics by assuming gas composition and temperature

ideally in homogeneous manner. The results of this model normally shows great different between numerical and experiment data.

Advantage on multi zone model is the input of temperature and gas compositions able to be treated independently as size geometry of whole cylinder in actual application is not in simplest one. Especially for the complicated geometry of cylinder, gas flow and aerodynamics affect gas composition, therefore, dissimilar in between different location at one particular time.

In this chapter, a numerical analysis conducted to re-demonstrate behavior of LTO which invariably start a lower region of equivalence ratio and ignition point of thermal heat varies based on magnitude of fuel concentration gradient. A simple geometry model was used in this study with different zone and each zone set to be in same size. Early stage of simulation, a 33 zone were set to investigate behavior of LTO and thermal flame in detail. However number of zone was reduced to 9 zone in this study for lesser time consuming purpose. Effect of the peak pressure and heat release between at these reduced model was compared, and no significant differents were observed.

6.2 Simulation condition

The numerical calculation software used in this study, CHEMKIN is a software that commonly used for solving problems regarding chemical kinetics especially in combustion and chemical processing fields. Reaction mechanism used in calculation was developed by Lawrence Livermore National Laboratory (LLNL) for n-heptane as primary reference fuel, based on experimental data reported by (Curran *et al.* 1998).

A multi zone reactor model was selected due to its ability to simulate different gradient in a particular zone either for temperature gradient or fuel-oxidizer chemical species gradient. In the actual experiment, five different location in cylinder were selected for measurement of local fuel concentration gradient, however in this simulation the whole cylinder was divided into nine different zones in one model. In each zone, temperature and chemical species (in molar basis) can be set independently therefore appropriate data needed for simulation purpose. By referring to Figure 3.8, growth of FCG in cylinder developed in exponential manner, however for simplification purpose the growth of FCG

in simulation throughout 9 zones were assumed to be in linear manner. Three different magnitude of FCG was selected to be reported in this study and detail of chemical species and its fraction (molar basis) was listed in Figure 6.1.

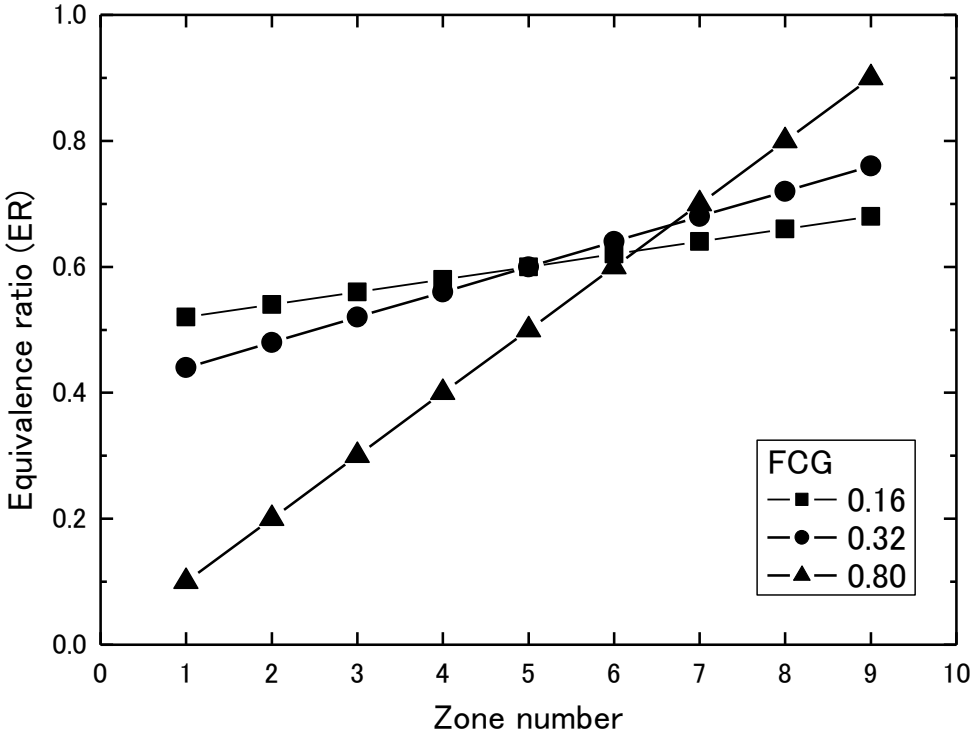

Figure 6.1 Magnitude of fuel concentration gradient applied in simulation

Chemical species in each layer were nitrogen, oxygen, carbon dioxide (4%vol) and n-heptane and its fraction were differs based on corresponding ER. Another important parameter to be considered in this model is the temperature at TDC. To maintain simplification of model, temperature at TDC were calculated by assuming compression complete in adiabatic manner, based on initial pressure, Pi and initial temperature, Ti used in the experiment. Therefore, the temperature at TDC used in this simulation were a bit higher compared with experimental data. Engine displacement volume and clearance volume were set to be 471 cm^3 and 48 cm^3 so that the compression ratio to be approximately 11. As RCM was used in the experiment, this model also applied same

concept that gas mixture being adiabatically compressed to the value of P_{TDC}, and the volume of cylinder maintained unchanged.

6.3 Simulation result

Characteristic of LTO and hot flame able to demonstrate by monitoring increment of temperature in the zone. For better visualization purpose, the temperature increment in each zone was plot in 3D graph, as can be seen in Figure 6.2. Zone number, elapsed time (ms) and gas temperature (K) plotted on X, Y & Z axes respectively. Zone number 1 indicate the uppest region (the leanest ϕ), until zone number 9 refer to the lowest region in cylinder (the richest ϕ). Elapsed time (ms) in these graphs refer to simulation time after TDC condition (TDC = 0 ms). Temperature value plotted here indicates for overall gas temperature for each zone, which the range of temperature plot was fixed to be from 0 – 3000 K. As shown in Figure 5.2, two times pressure increment due to two-stage ignition process was noticeable. However, in temperature plot graph as shown in Figure 6.2, first stage ignition exhibit temperature to be between 850 K – 1000 K (indicate by light dark blue color), and denote as first temperature increment in the figure. While for second stage ignition, the exhibited temperature was starting from 2000 K – 2200 K which shown in second temperature increment. The temperature range for first and second stage ignition was decided by compared simultaneously simulation result of pressure profile and temperature profile, which conducted in homogeneous manner.

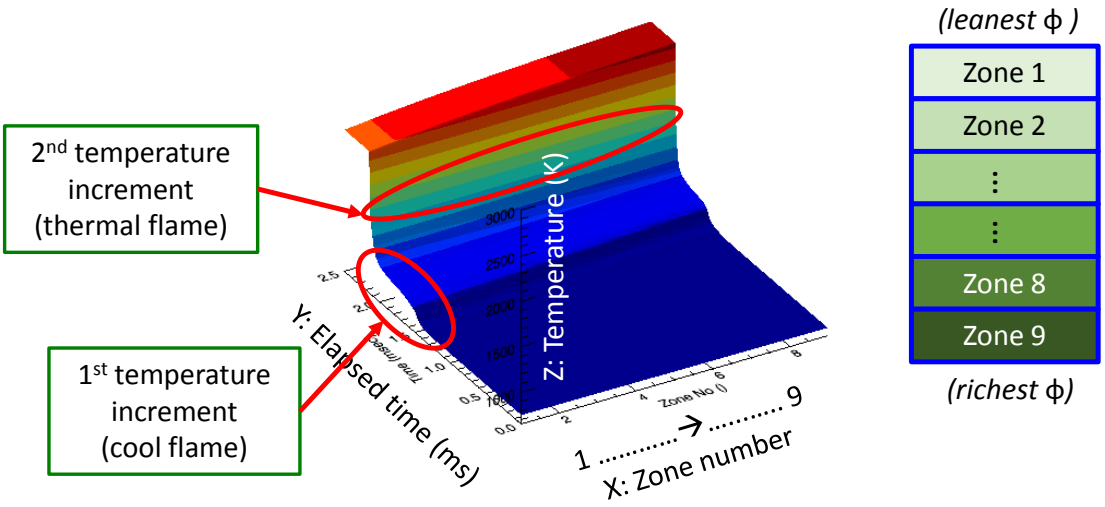

Figure 6.2 Detail explanation of temperature plot

Simulation in multi zone model done for three FCG conditions as in Figure 6.1 with pressure at TDC was fixed to be 2.62 MPa, and temperature at TDC were differs based on local ER. The temperature at TDC was calculated by assuming compression complete in adiabatic manner.

Simulation results for all condition mentioned above was shown in Figure 6.3. In this figure, pressure profiles and correlated temperature plot was shown. Elapsed time for temperature plot shown here was for the condition combustion complete in equal volume. In all figures, two times increment were observed with the first increment recorded temperature approximately 900K-1000K and temperature after second increment depend on simulation condition in each zone. In all condition also, first increment at lower zone number (upper region in the model) was earlier than middle and higher zone number (lower region in the model). This behavior was similar to the behavior of increment in cylinder during measurement temperature in experiment therefore it was proved that, the higher temperature of mixture gas at TDC then LTO would take place earlier. Moreover, as magnitude of FCG was increased, maximum temperature at upper region was demolished due to local equivalence ratio at upper region was too lean. Therefore, complete combustion was hard to achieve even temperature at upper region was set higher. The phenomenon was obvious in Figure 6.3(c).

Based on all pressure profiles in Figure 6.3, two-stage ignition successfully demonstrated for condition FCG 0.16 and FCG 0.32. However, as magnitude of FCG become larger as FCG 0.80, the first peak of first stage ignition getting harder to be observe. This phenomenon also identical with experiment data which is shown in Figure 5.4. Zone number 1 in temperature plot in Figure 6.3(c) shows that the temperature increased in gradual pattern until approximately 2.3 ms, then experience first stage temperature increment. However, at the same moment at zone number 6 – 9, second stage temperature increment occurred. It understood here that, when second stage appears at higher zone number, the first stage temperature increment was not complete yet in all zone. This may contribute to the fact that the peak of first stage ignition in FCG 0.80 in Figure 6.3 (c) was hard to distinguish. Although there was first stage of temperature increment in zone number 1 - 3 in FCG 0.80 observed at 2.4 ms, further elapsed time in particular zone number also shows that no second temperature increment appeared. The equivalence ratio set in the zone was below than 0.3. Thus, the equivalence ratio here was too low to complete auto-ignition combustion.

The pressure traces for FCG 0.32 and 0.80 start to increase earlier compare with FCG 0.16, however, rise gradually therefore consume longer time to reach peak pressure for both first and second stage ignition. Maximum pressure on the other side shows reverse effect that were reduced with increasing magnitude of FCG. From the Figure 6.3, maximum pressure reduces a bit for FCG 0.32, however for FCG 0.80, the maximum pressure drastically reduced.

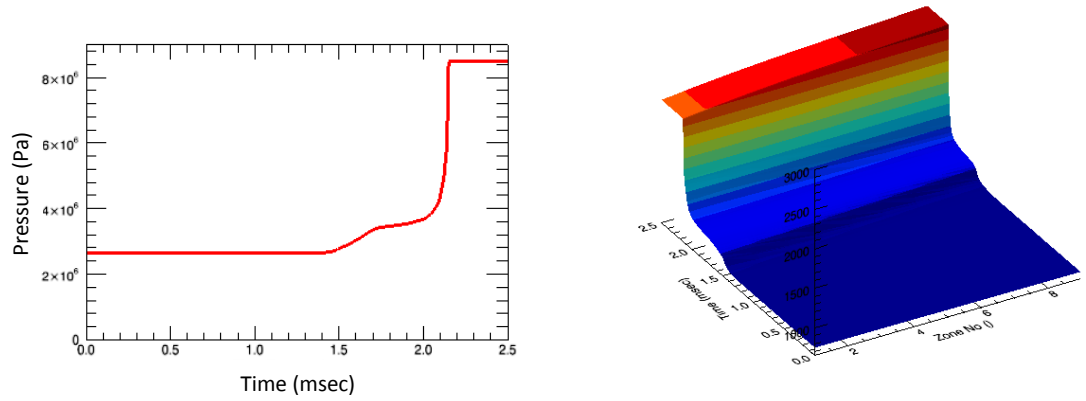

a) FCG 0.16

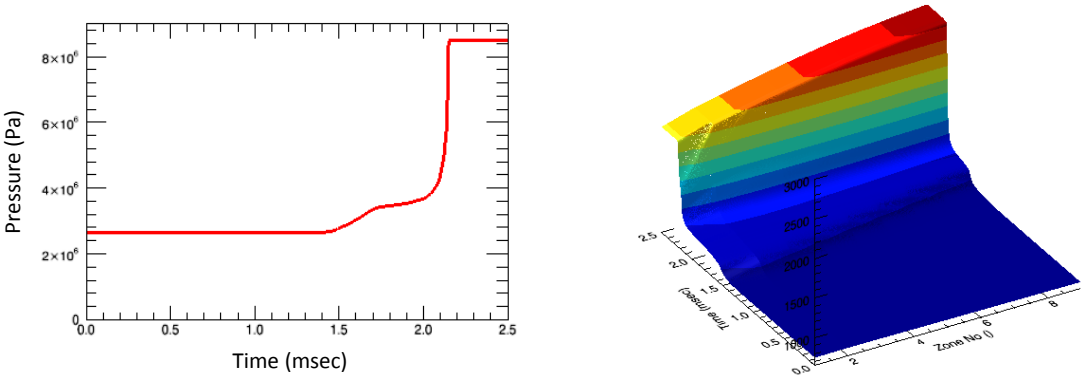

b) FCG 0.32

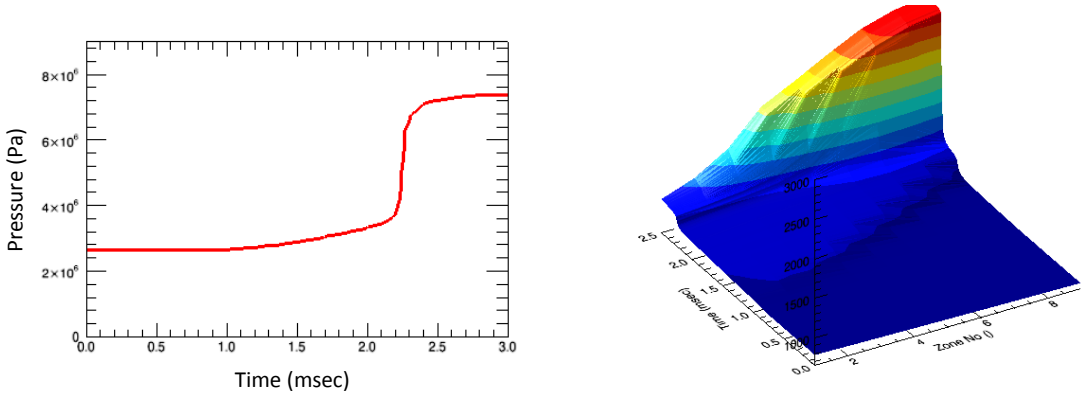

c) FCG 0.80

Figure 6.3 Temperature distribution profile for different magnitude of FCG

Simulation condition FCG 0.16 is expected to be near homogeneous condition. Comparison of pressure profiles between homogeneous and FCG=0.16 shows that pressure of the one with gradient rise as earlier at 1.5 ms. From Figure 6.4(a), temperature at zone 1 start to increase about 10-20 K from initial temperature. As time elapsed further, temperature at other zone increase in sequence from zone 1 to zone 9, and completed within approximately 0.3 ms which can be observed from Figure 6.4(c). As time elapsed further until up to 2.0 ms Figure 6.4(e), temperature inside model increase with a very slow rate. The temperature increment pattern was tally with pressure traces increment pattern shown in pressure profile located above in Figure 6.4. It also can be noticed that pressure trace start to increase significantly between 2.1 – 2.2 ms, and the correlated temperature history are shown in Figure 6.4 (f) – (i). Within this short period, thermal flame was assumed to ignite here therefore maximum pressure over 7 MPa was achieved after that period.

Another thing to be stressed here that for FCG 0.16, second temperature increment start to increase at somewhere between zone 1-3, approximately at 2.14 ms (Figure 6.4(f). During this period, temperature at zone 1-3 increase about 1100 to 1500 K. Temperature at another zone also increase in the next sequence of elapsed time within in short period, therefore spread of the second temperature increment was not by the thermal flame spread but by the successive of various of ignition point, from in the combustion chamber.

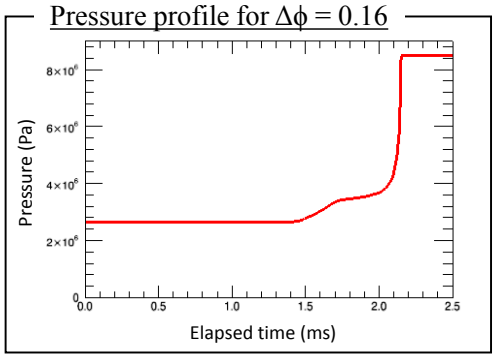

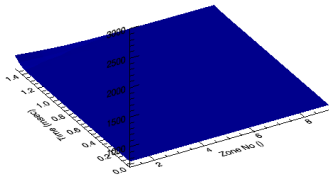

a) 0 - 1.50 ms

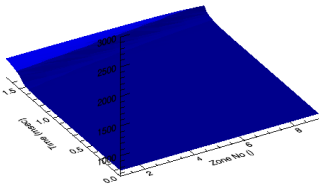

b) 0 - 1.70 ms

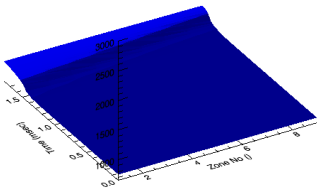

c) 0 - 1.80 ms

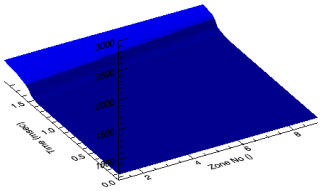

d) 0 - 1.90 ms

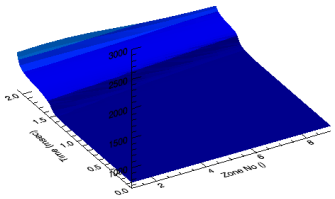

e) 0 – 2.10 ms

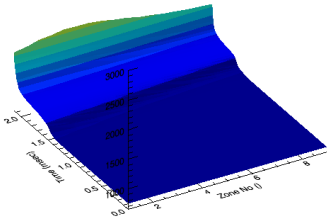

f) 0 – 2.14 ms

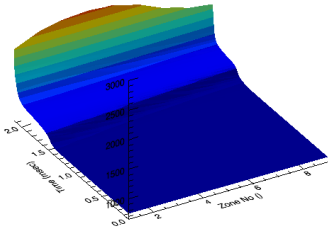

g) 0 – 2.145 ms

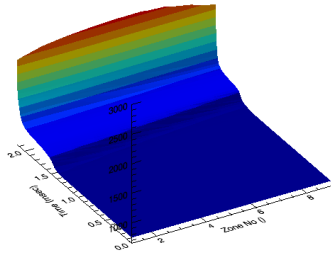

h) 0 – 2.148 ms

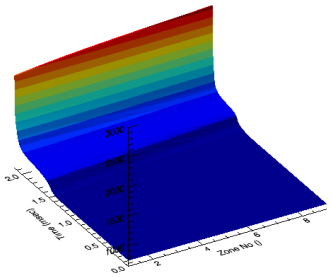

i) 0 – 2.16 ms

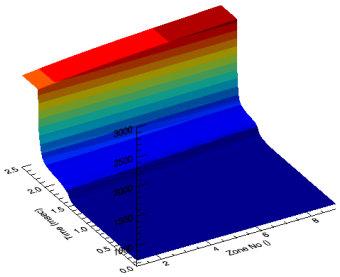

j) 0 – 2.50 ms

Figure 6.4 Temperature profile growth for FCG=0.16

Figure 6.5 shows pressure profile and temperature plot profiles for simulation condition with FCG = 0.32. Pressure start to rise earlier compare with FCG = 0.16 as early at approximately 1.4 ms but with a slower rate. Rate of pressure increment (inclination of dP/dt) reduce compare with FCG 0.16 and different time of first temperature increment between zone 1 and zone 9 become larger. If the first temperature increment to be interpreted as cool flame in experiment, then it is observed that cool flame take longer time to move from upper region to lower region. When elapsed time proceed up to 2.13 ms (Figure 6.5(d), temperature start to increase at faster rate at middle zone which the temperature recorded at middle zone during the time was between 1100 – 1500 K. As time elapsed further, temperature increase in another zone like simultaneously spread from center region to upper and lower region of simulation model. Maximum pressure in this simulation was not differed too much with previous simulation condition although it takes a little time to reach peak pressure. Overall for FCG 0.32, cool flame can be observed start from upper region spread to the downward region while the hot flame was first ignited at the middle zone number and then followed by neighbor region.

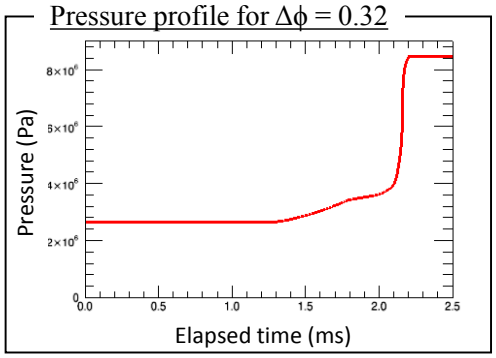

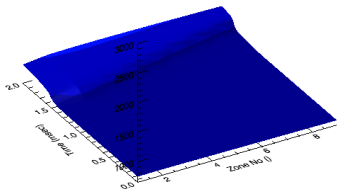

a) 0 – 2.00 ms

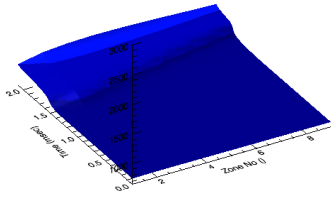

b) 0 – 2.10 ms

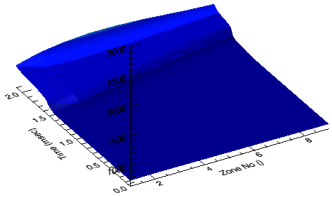

c) 0 – 2.12 ms

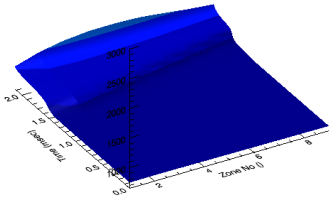

d) 0 – 2.13 ms

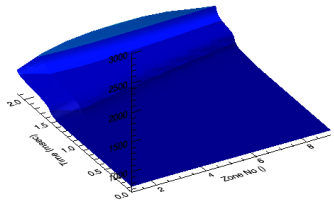

e) 0 – 2.14 ms

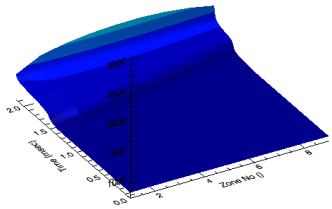

f) 0 – 2.15 ms

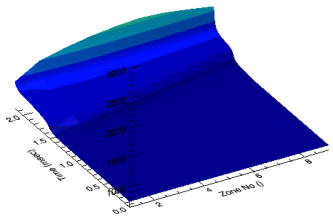

g) 0 – 2.16 ms

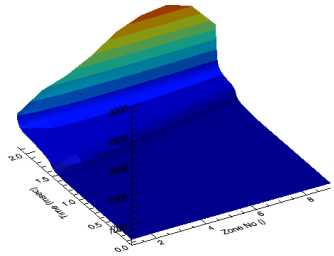

h) 0 – 2.17 ms

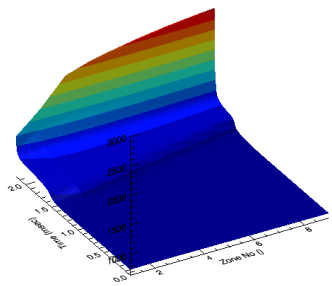

i) 0 – 2.18 ms

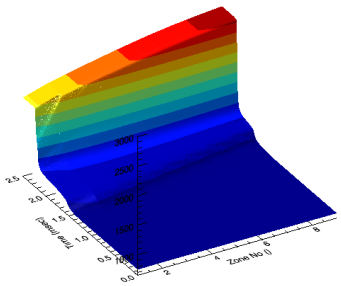

j) 0 – 2.50 ms

Figure 6.5 Temperature profile growth for FCG=0.32

For simulation condition of FCG = 0.80, pressure profile and its temperature plot profile shows in Figure 6.6. First increment in pressure profile observed start as earlier from 1.0 ms. However, unlike from other FCG condition, first temperature increment start to observe not at zone 1 but zone 2. It is quite interesting that it takes up to 1.5 ms for temperature in zone 1 to increase up to 10 – 20 K from initial temperature. Even initial temperature at zone 1 was set high as up to 780 K, the equivalence ratio of 0.1 at zone 1 was too lean therefore chemical kinetics takes longer time to react and to release significant amount of heat. The reason of lower maximum pressure achieved in FCG 0.80 was explained earlier.

First temperature increment of cool flame was in the same pattern with other experiment condition. However for the second temperature increment, or hot flame was found to be ignited at lower region (zone number 8 - 9), and then shift upwards of combustion chamber. The simulation result obtained for FCG 0.80 same with high magnitude of FCG in experiment, which was FCG $\geq$ 0.86. ($t_w \leq 100$ s).

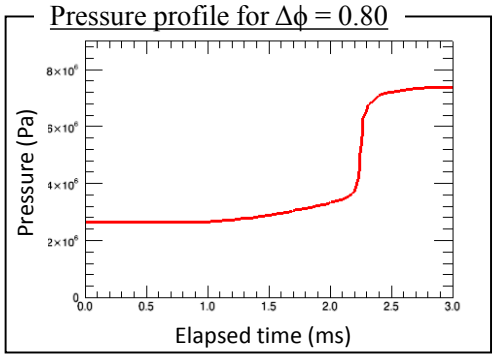

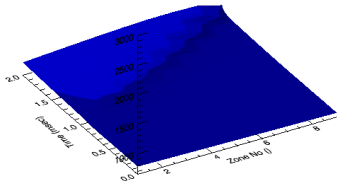

a) 0 – 2.00 ms

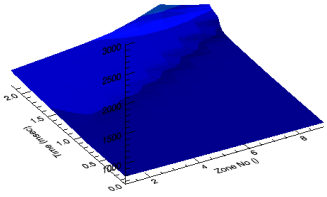

b) 0 – 2.20 ms

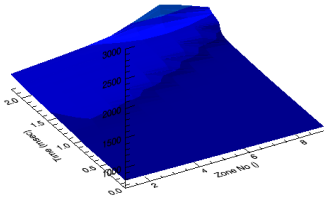

c) 0 – 2.21 ms

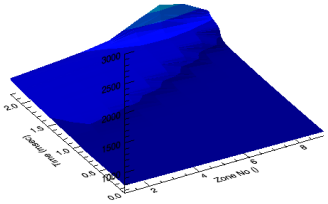

d) 0 – 2.22 ms

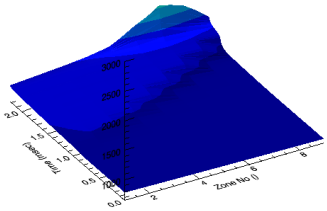

e) 0 – 2.23 ms

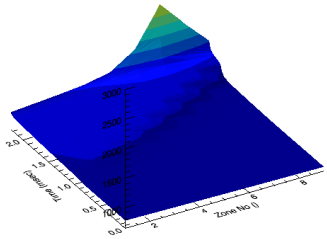

f) 0 – 2.24 ms

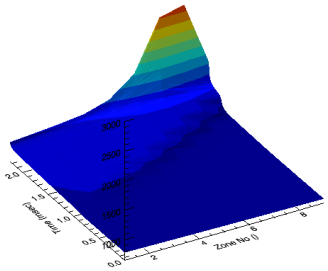

g) 0 – 2.25 ms

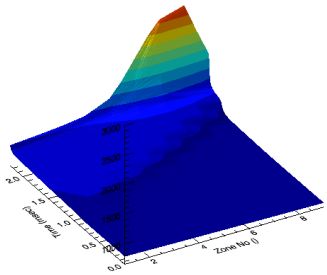

h) 0 – 2.26 ms

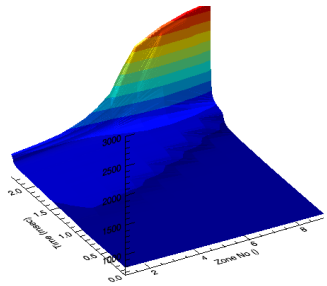

i) 0 – 2.29 ms

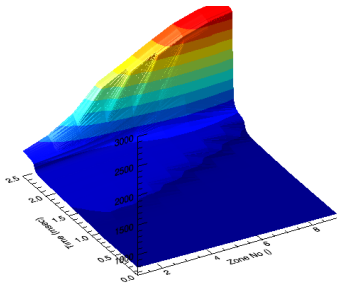

j) 0 – 2.50 ms

Figure 6.6 Temperature profile growth for FCG=0.80

7. Conclusion

7.1 Chapter overview

In this chapter, summarized conclusion from discussion of experimental results and data analysis of experiment and also conclusion from simulation results. Experiment conducted for condition where equivalence ratio in cylinder measured in horizontal layer were set to be homogeneous and increasing gradient. The summary has been divided into three segments.

7.2 Temperature distribution measurement in auto-ignition process

Non-intrusive temperature measurement method was favorable in this study. Experimental study conducted in a rapid compression machine by applying infrared emission method for temperature measurement with 4.3 μm band of carbon dioxide. Within conducted experiment, the following conclusion are being drawn:

1. For the cases of no combustion occurred (no-reacting charge), growth of temperature inside cylinder agreed with theoretical estimation. The result is also confirmed by varying parameter of compression ratio. The developed temperature measurement technique could distinguish the temperature difference about 10K. Additionally the characteristics temperature distribution due to the movement of the piston called a roll up vortex was successfully captured. The results showed that temperature at roll up vortex region was 10-30K lower than the core temperature.

2. The temporal behavior of the temperature profile of the reacting charge in the cylinder during the ignition delay was successfully captured. Not only the temperature change due to the appearance of cool flame but also the gradual temperature increasing during the low temperature reaction were captured quantitatively as two-dimensional information. Such information is useful for interpret the auto-ignition phenomena of the compressed charge.

7.3 Behavior of temperature profile of auto-ignition with fuel concentration gradient

Effect of applying fuel concentration gradient was investigated experimentally. The FCG was created by injecting liquid n-heptane carefully from the bottom part of the cylinder. Temperature distribution inside cylinder was measured with aid of a high-speed infrared camera and able to be viewed as image temperature. The following conclusion are obtained;

1. Applying FCG in the cylinder prior the compression, temperature distribution also created in the charge after the compression. The compressed charge had high temperature at the leaner Ø part and low temperature at the richer Ø part of the cylinder due to the difference in ratio of specific heats. The developed temperature measurement technique could capture the temperature profile in the compressed charge.

2. Due to the temperature distribution, cool flame started from the leaner Ø part and moved to the richer Ø part. In all conditions conducted, the cool flame started from the leaner part and the low temperature oxidation occurred in the stratified charge successively. The pressure rise due to the low temperature oxidation became gradual due to the stratified ignition delay.

3. After the stratified ignition of low temperature oxidation, relatively large temperature difference remained in the charge, and then the high temperature oxidation started. The starting point of the hot flame depended on the magnitude of ΔØ of FCG. When ΔØ was small, the hot flame moved from top to bottom as well as cool flame. When ΔØ was large, the hot flame moved from bottom to top in contrast. There was a critical $\Delta Ø_{,cr}$, in which the total ignition delay at each local point became close to the same.

4. The stratified occurrence of high temperature oxidation reduced the knock intensity, KI. With increasing ΔØ, the KI first decreased, but then increased at $\Delta Ø_{,cr}$. Further increasing ΔØ, KI decreased again, but too large ΔØ caused incomplete combustion, which resulted in lower maximum pressure.

7.4 Simulation on auto ignition in cylinder by applying fuel concentration gradient

The effort to simulate auto ignition process in cylinder by applying fuel concentration gradient (FCG) been carried with aid of numerical calculation software, CHEMKIN which being almost used in solving problems regarding chemical kinetics. Three different value of FCGs were simulated and compression ratio to be set at 11. Based on the simulation result, following conclusion are obtained;

1. Similar pattern on pressure traces between experimental and simulation results able to be collected. Lower magnitude of FCG elicited longer

ignition delay and higher maximum pressure. At highest of FCG, pressure trace gradually increase and maximum pressure was demolished.

2. Development of first stage ignition is able to be viewed from first stage temperature increment. The timing of first stage ignition is shortest in leanest of local equivalence ratio. This behavior was anticipated with theoretical assumption that assume leaner equivalence ratio exhibit higher temperature after being adiabatically compressed.

3. In all cases of FCG, first stage ignition invariably starts from leaner part of local equivalence ratio, then followed by next nearest zone. Its explain behavior of cool flame start from upper side cylinder in experiment then moving downwards to bottom cylinder. However, depend on the value of local equivalence ratio not all are guaranteed to experience second stage ignition (hot flame) although first stage ignition occurred in the particular zone. Incomplete combustion in a zone affects overall pressure in cylinder to be drastically demolished.

4. The ignition point of hot flame or second stage ignition are independent with FCG. However in simulated FCG, three different ignition point of hot flame observed in experiment were successfully demonstrated. Since the ignition timing of hot flame was closed between each region, it suggested that the movement of the hot flame not be from flame propagation but the succession of auto-ignition phenomena.

Bibliography

Agnew, W.G., 1961. *End Gas Temperature Measurement by a Two-Wavelength Infrared Radiation Method*. SAE Trans.

Agnew, W.G.G., Agnew, J.T.T., and Wark, K., 1955. Infrared Emission from Cool Flames Stabilized Cool Flames; Engine Cool Flame Reactions; Gas Temperatures Deduced from Infrared Emission. *Symposium (International) on Combustion*, 5 (1), 766–778.

Blunsdon, C.A., Dent, J.C., and Malalasekera, W.M.G., 1993. Modelling Infrared Radiation from the Combustion Products in a Spark Ignition Engine.

Buono, D., Iarrobino, E., and Senatore, A., 2011. Optical Piston Temperature Measurement in an Internal Combustion Engine. *SAE International Journal of Engines*, 4 (1), 2011–01–0407.

Clarkson, J., Griffiths, J.., MacNamara, J.., and Whitaker, B.., 2001. Temperature Fields During the Development of Combustion in a Rapid Compression Machine. *Combustion and Flame*, 125 (3), 1162–1175.

Curran, H.J., Gaffuri, P., Pitz, W.J., and Westbrook, C.K., 1998. A Comprehensive Modeling Study of n-Heptane Oxidation. *Combustion and Flame*, 114 (1-2), 149–177.

Desgroux, P., Gasnot, L., and Sochet, L.R., 1995. Instantaneous Temperature Measurement in a Rapid-Compression Machine using Laser Rayleigh Scattering. *Applied Physics B Laser and Optics*, 61 (1), 69–72.

Desgroux, P., Minetti, R., and Sochet, L.R., 1996. Temperature Distribution Induced by Pre-lgnition Reactions in a Rapid Compression Machine. *Combustion Science and Technology*, 113 (1), 193–203.

Griffiths, J.., MacNamara, J.., Sheppard, C.G.., Turton, D.., and Whitaker, B.., 2002. The Relationship of Knock During Controlled Autoignition to Temperature Inhomogeneities and Fuel Reactivity. *Fuel*, 81 (17), 2219–2225.

Grosshandler, W.L., 1993. *RADCAL - a Narrow-Band Model for Radiation Calculations in a Combustion Environment*. Gaithersburg, MD.

Hamamoto, Y., Tomita, E., and Jiang, D., 1994. Temperature Measurement of End Gas under Knocking Condition in a Spark-Ignition Engine by Laser Interferometry. *JSAE Review*, 15 (2), 117–122.

Ihara, T., Qin, X., Tanaka, T., and Wakai, K., 2007. Auto Ignition and Knocking Phenomena in Stratified Mixture of Lean Condition. *In*: *ASME/JSME 2007 Thermal Engineering Heat Transfer Summer Conference, Volume 1*. ASME, 597–600.

Iijima, A., Yoshida, K., and Shoji, H., 2010. Optical Measurement of Autoignition and Combustion Behavior in an HCCI Engine. *SAE International Journal of Engines*, 3 (2), 2010–32–0089.

Jir-Ming, C. and Jun-Hsien, Y., 1996. The Measurement of Open Propane Flame temperature using infrared technique. *Journal of Quantitative Spectroscopy and Radiative Transfer*, 56 (1), 133–144.

Kamarrudin, N.S., Tanaka, S., Takahashi, S., and Ihara, T., 2013. Measurement of Temperature Profile during Ignition Delay in the Cylinder with Fuel Concentration Gradient. *In*: *9th Asia-Pacific Conference on Combustion*.

Liu, H., Zhang, P., Li, Z., Luo, J., Zheng, Z., and Yao, M., 2011. Effects of Temperature Inhomogeneities on the HCCI Combustion in an Optical Engine. *Applied Thermal Engineering*, 31 (14-15), 2549–2555.

MALKMUS, W., 1963. Infrared Emissivity of Carbon Dioxide (43-μ Band). *Journal of the Optical Society of America*, 53 (8), 951.

Mansfield, a. B., Wooldridge, M.S., Di, H., and He, X., 2015. Low-Temperature Ignition Behavior of Iso-Octane. *Fuel*, 139, 79–86.

Mattison, D.W., Jeffries, J.B., Hanson, R.K., Steeper, R.R., De Zilwa, S., Dec, J.E., Sjoberg, M., and Hwang, W., 2007. In-Cylinder Gas Temperature and Water Concentration Measurements in HCCI Engines using a Multiplexed-Wavelength Diode-Laser System: Sensor Development and Initial Demonstration. *Proceedings of the Combustion Institute*, 31 I, 791–798.

McComiskey, T., Jiang, H., Olan, Y., Rhee, K.T., and Kent, J.C., 1993. High-Speed Spectral Infrared Imaging of Spark Ignition Engine Combustion. *In*: *International Congress & Exposition*.

Minetti, R., Carlier, M., Ribaucour, M., Therssen, E., and Sochet, L.R., 1995. A Rapid Compression Machine Investigation of Oxidation and Auto-Ignition of n-Heptane: Measurements and Modeling. *Combustion and Flame*, 102 (3), 298–309.

Mittal, G. and Sung, C.-J., 2006. Aerodynamics Inside a Rapid Compression Machine. *Combustion and Flame*, 145 (1-2), 160–180.

Modest, M.F., 2003. *Radiative Heat Transfer, 2nd Ed., Academic Press, New York*.

Modest, M.F. and Bharadwaj, S.P., 2002. Medium Resolution Transmission Measurements of CO2 at High Temperature. *Journal of Quantitative Spectroscopy and Radiative Transfer*, 73 (2-5), 329–338.

Moroto, M., Wakai, K., Takahashi, S., and Shimizu, S., 1999. Two-Dimensional Temperature Distribution Measurement of Combustion Gas by an Infrared 2-Band Absorption CT Employing CO2: Experimental Investigations of Selected Wave Number and Measurement Accuracy. *Combustion Science and Technology (in Japanese)*, 6 (3), 161–170.

Nagae, T., Takahashi, S., Ihara, T., Wakai, K., and Urata, Y., 2006. Effect of Selecting Infrared Band on Temperature Measurement in Cylinder using Infrared Pyrometry. *In*: *44th Symposium (Japanese) on Combustion (in Japanese)*. 42–43.

Peterson, B., Baum, E., Böhm, B., Sick, V., and Dreizler, A., 2013. High-speed PIV and LIF Imaging of Temperature Stratification in an Internal Combustion Engine. *Proceedings of the Combustion Institute*, 34 (2), 3653–3660.

Qin, X., 2007. Study on Knocking Phenomenon in Stratified Mixture. Gifu University.

Rieker, G.B., Li, H., Liu, X., Liu, J.T.C., Jeffries, J.B., Hanson, R.K., Allen, M.G., Wehe, S.D., Mulhall, P.A., Kindle, H.S., Kakuho, A., Sholes, K.R., Matsuura, T., and Takatani, S., 2007. Rapid Measurements of Temperature and H2O Concentration in IC Engines with a Spark Plug Mounted Diode Laser Sensor. *Proceedings of the Combustion Institute*, 31 (2), 3041–3049.

Saifullah, N., Takahashi, S., and Ihara, T., 2015. Temperature Distribution Measurement during Low Temperature Reaction in Auto-ignition Process. *Journal of Combustion Society of Japan*, 57 (179), 82–89.

Silverman, S., 1949. The Determination of Flame Temperatures by Infrared Radiation. ... *on Combustion and Flame, and Explosion Phenomena*, 3 (1), 498–500.

Singh, S., Musculus, M.P.B.B., and Reitz, R.D., 2009. Mixing and Flame Structures Inferred from OH-PLIF for Conventional and Low-Temperature Diesel Engine Combustion. *Combustion and Flame*, 156 (10), 1898–1908.

Tanaka, S., 2003. Two-stage Ignition in HCCI Combustion and HCCI Control by Fuels and Additives. *Combustion and Flame*, 132 (1-2), 219–239.

Thirouard, B., Cherel, J., and Knop, V., 2005. *Investigation of Mixture Quality Effect on CAI Combustion*.

Xiaojian, Q., Kazunori, W., Tadayoshi, I., and Kentaro, S., 2006. Study on Knocking Phenomenon in Stratified Mixture. *Journal of the Combustion Society of Japan*, 48 (146), 363–371.

Yamada, H., Yoshii, M., and Tezaki, A., 2004. A Chemical Mechanistic Analysis on Compression Ignition Process of Straight Chain Alkanes. *In*: *Fuels & Lubricants Meeting & Exhibition*.

Yao, M., Zheng, Z., and Liu, H., 2009. Progress and Recent Trends in Homogeneous Charge Compression Ignition (HCCI) Engines. *Progress in Energy and Combustion Science*, 35 (5), 398–437.

Yuen, F.T.C. and Gülder, Ö.L., 2009. Premixed Turbulent Flame Front Structure Investigation by Rayleigh Scattering in the Thin Reaction Zone Regime. *Proceedings of the Combustion Institute*, 32 (2), 1747–1754.

Zhao, H., Collings, N., and Ma, T., 1991. The Cylinder Head Temperature Measurement by Thermal Imaging Technique. *In*: *SAE transactions*.